cells were maintained in RPMI1640 medium supplemented with 10% fetal bovine serum, 50 μM 2-mercaptoethanol, 2.0 mM L-glutamine and 100 U/ml IL-3. Lenalidomide (10 μM) or 0.01% DMSO were added daily during the experiments. Human myeloid leukemia cell lines carrying del(5q), HL-60 and KG-1 were also used. Cell growth was assessed by counting the number of living cells. The morphological assessment was performed with May–Gruenwald–Giemsa stained cytospin slides.

Apoptosis assay

The apoptosis was examined using AnnexinV Apoptosis Detection Kit (BD Pharmingen, San Diego, CA, USA) and all samples were analyzed by FACS Calibur flow cytometer and CellQuest software(Becton Dickinson, Franklin Lakes, NJ, USA).

Immunofluorescence study

MDS-L cells were centrifuged onto cytospin slides and fixed for 30 s in 4% formalin/50% acetone, then permeabilized with lysis buffer including 0.2% Triton X-100, 25 mM HEPES, 60 mM PIPES, 10 mM EGTA and 2 mM $MgCl_2$ for 30 s. Antibody staining was performed using mouse monoclonal anti-aurora kinase A (BD biosciences, San Jose, CA, USA), rabbit polyclonal anti-CDC25C(Santa Cruz Biotechnology, Santa Cruz, CA, USA) to detect centrosomes,[23] and AlexaFluor488- or AlexaFluor594-conjugated anti-IgG antibodies (Molecular Probes, Eugene, OR, USA) as secondary antibodies. The nucleus was stained with DAPI (Dojindo, Kumamoto, Japan). Cells were observed under an Olympus BX51 fluorescence microscope and a ×100/1.35 numerical aperture oil objective.

Live cell imaging by a time-lapse microscopy

Cells were seeded in 35 mm glass bottom culture dish and then 100 ng/ml Hoechst 33342 Dojindo was added for 1 h. Time-lapse imaging was performed on Zeiss Axiovert 200 M microscope (Zeiss, Göttingen, Germany) equipped with halogen light source, xenon lump, C4742-95ER digital camera and the Aquacosmos/ratio imaging system (Hamamatsu photonics K.K., Hamamatsu, Japan) at 37 °C and 5% CO_2. All images were collected using Zeiss Ph2 plan-NEOFLUAR ×40, 0.75 numerical aperture objective. Camera binning was 2 × 2, imaging times were 240 ms. Each image was captured every 2 min until the time points as indicated.

Cell-cycle and DNA ploidy analyses

Cells were fixed with 100% methanol for 60 min and treated with 2 mg/ml ribonuclease A (Nacalai Tesque, Kyoto, Japan) for 20 min at 37 °C, next with 50 μg/ml propidium iodide (PI; Sigma, St Louis, MO, USA) for further 20 min at room temperature. As to the analysis using bromodeoxyuridine (BrdU) and 7-amino-actinomycinD (7-AAD), the cells were pulse-labeled with 10 μM BrdU for 120 min and the cell-cycle assay was performed using BrdU Flow Kit (BD Pharmingen) and FACS Calibur flow cytometer. DNA ploidy was analyzed by the use of a laser-scanning cytometry as previously described.[24] Briefly, the cytospin samples stained with May–Gruenwald–Giemsa were captured with a CCD camera and their coordinates (x and y) on the slide were recorded. Next the identical smears were treated with 2 mg/ml ribonuclease A for 1 h at 37 °C and restained with 100 μg/ml PI, and the fluorescence intensity of each cell was quantified as the DNA contents together with the morphological assessment.

Statistical analyses

To compare the two nuclei of binucleated cells, we measured the surface area and DNA ploidy of each nucleus and calculated the Pearson product–moment correlation coefficients and the Sperman rank correlation coefficients.

Gene expression profiling

Gene expression profiling of MDS-L cells was examined in three independent experiments (lenalidomide-treated or DMSO-treated cells were harvested once on day 7 and twice on day 9). Total RNA was extracted with RNeasy Mini Kit (Qiagen, Germantown, MD, USA) and 5 μg of total RNA was amplified with the one-cycle cDNA synthesis and the one-cycle Target Labeling and Control Reagent packages (Affymetrix Santa Clara, CA, USA). Biotin-labeled fragmented cDNA was hybridized to Affymetrix-GeneChip Human Genome U133 Plus 2.0 Arrays covering >47,000 transcripts representing 39,000 human genes. Chips were washed and scanned with a GeneChip Scanner 3000 (Affymetrix).

Reverse transcription–polymerase chain reaction (RT–PCR)

Total RNA was extracted with RNeasy Mini Kit (Qiagen) and RT–PCR was performed using One step RNA PCR Kit (TAKARA BIO, Otsu, Japan) and following primers: *non-muscle myosin heavy-chain10(MYH10)* (sense:CATCTACAACCCTGCCACTC; antisense:TCCTCACGATCTTGAAGCATG), *aurora kinase B(AURKB)* (sense:ATGGCCCAGAAGGAGAACTC; antisense:TTCTCCCG AGCCAAGTACAC), *polo like kinase* (sense:ATGAGTGCTGCA GTGACTGC; antisense:GAGCAGCAGAGACYYAGGCA), *kinesin family member 20A* (*KIF20A*)(sense:CTAAATTACAGCAGTG CAAAGCAG; antisense:TTAGTACTTTTTGCCAAAAGGCCCAG), *CDC14A*(sense:CTCCATCGATGAGGAGCTGG; antisense:GAC AGGAGTGCTCTGTAGGC), *SPARC* (sense:CTGTGGCAGAGGT GACTGAG; antisense:GGCAGGAAGAGTCGAAGGTC), *glyceraldehydes-3-phosphate dehydrogenase (GAPDH)* (sense:GCC TCCTGCACCACCAACTG; antisense:CCCTCCGACGCCTGCTT CAC). PCR was performed using GeneAmp PCR system 9700 (Applied Biosystems, Tokyo, Japan) for 30 cycles, each consisting of 30 s at 94 °C, 30 s at 58 °C and 30 s at 72 °C.

Immunoblotting analysis

Cell lysates of MDS-L were prepared in lysis buffer containing 50 mM Tris-HCL, 150 mM NaCl, 5 mM EDTA, 0.5% TritonX-100, 0.05% sodium dodecyl sulfate (SDS), 0.5% sodium deoxycholate, 2 mM phenylmethylsulfonyl fluoride and 1 mM Na3VO4. Cell lysates were separated in SDS–polyacrylamide gel electrophoresis (SDS–PAGE) and immunoblotting analysis was performed as previously described.[25] Used primary antibodies were rabbit anti-KIF20A(Bethyl Laboratories, Montgomery, TX, USA) and mouse anti-aurora kinase B(BD Biosciences, San Jose, CA, USA).

Results

Treatment with lenalidomide inhibits the proliferation of MDS-L cell line

As lenalidomide is reported to inhibit the growth of CD34-positive cells with del(5q)[7] or Burkitt lymphoma cell lines,[18] we investigated the effect of lenalidomide on the growth of myeloid cell lines carrying del(5q). Daily addition of lenalidomide to *in vitro* culture did not show any suppressive effect on HL-60

(Figure 1a) nor KG-1 (data not shown). In contrast, MDS-L cells proliferated in the presence of IL-3 by day 4, but after that the cell number was gradually decreased together with appearance of dying or dead cells (Figures 1a and 2a). We analyzed apoptosis by dual staining of annexinV and PI, and found that lenalidomide induces apoptotic cell death onto a major part of MDS-L cells after around day 5 (Figure 1b).

MDS-L cells become multinucleated and polyploid by the treatment with lenalidomide

Lenalidomide-induced apoptosis to most of MDS-L cells, and we also found that lenalidomide treatment brought about the appearance of binucleated cells on day 4 (before the beginning of massive cell death) and subsequently multinucleated cells were often detected. On day 10 about a half of the cells which survived under lenalidomide treatment represented multinuclearity (Figures 2a and b).

In general, cell division consists of the two-step process: nuclear division (mitotic division) and subsequent cytoplasmic division (cytokinesis). Disturbance of either division might give rise to multinucleated cells. To examine whether the chromosome segregation ordinarily occurs or not, we compared the size and DNA contents of two nuclei of more than 100 binucleated cells by photomicrographic measurement and laser-scanning cytometry, respectively, and confirmed that the two nuclei were almost of the same size (the correlation coefficient between the two nuclei was 0.827) and such cells proved to be certainly 4N. These data indicate that lenalidomide treatment does not impair the DNA synthesis and that the chromosome segregation is normally accomplished to generate equally binucleated cells.

Next, we analyzed the cell-cycle pattern and the DNA ploidy of lenalidomide-treated MDS-L cells by flow cytometry. The percentage of subdiploid (<2N) cells was increased and instead diploid (2N) cells were decreased after lenalidomide treatment (Figure 3a). Furthermore, the cells with polyploidy such as tetraploid (4N) on day 4, and subsequently hyperpolyploid cells

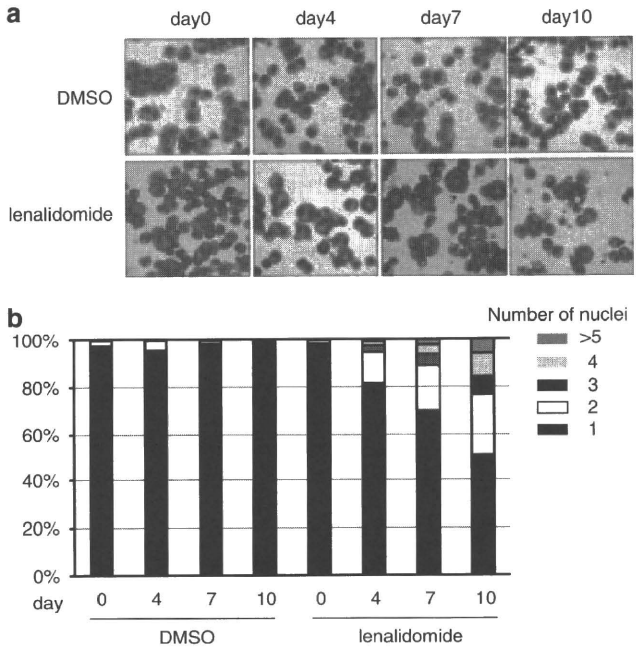

Figure 2 Lenalidomide induces the formation of multinuclearity in MDS-L cells. MDS-L cells were cultured in the presence of lenalidomide or DMSO as a control. (**a**) Morphological change of MDS-L cells during cultivation (May–Gruenwald–Giemsa stain). (**b**) The number of nuclei on each cell during cultivation (shown in percentage). Approximately 400 cells were counted on the indicated days.

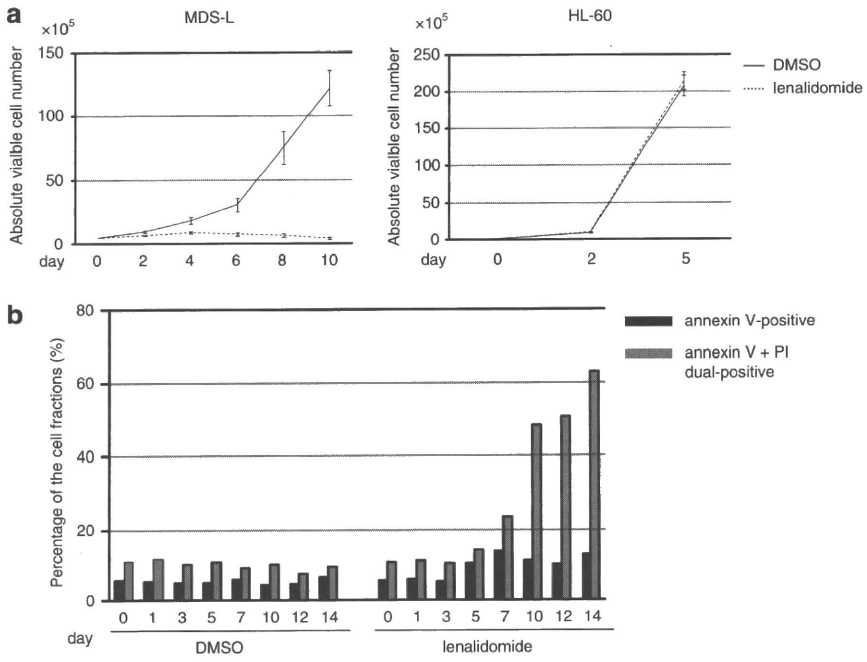

Figure 1 Lenalidomide inhibits the proliferation of MDS-L cells mainly by apoptosis. MDS-L and HL-60 cells were cultured in the presence of 10 μM lenalidomide or 0.01% DMSO as a control. (**a**) The cell number was counted on the indicated days. The data shown are the average ± s.d. of three independent experiments. (**b**) Apoptosis was assessed by flow cytometry using annexinV and propidium iodide (PI) staining on the indicated days. The percentages of only annexinV-positive cells (black column) and annexinV-PI dual-positive cells (gray column) are shown as the average of duplicate experiments.

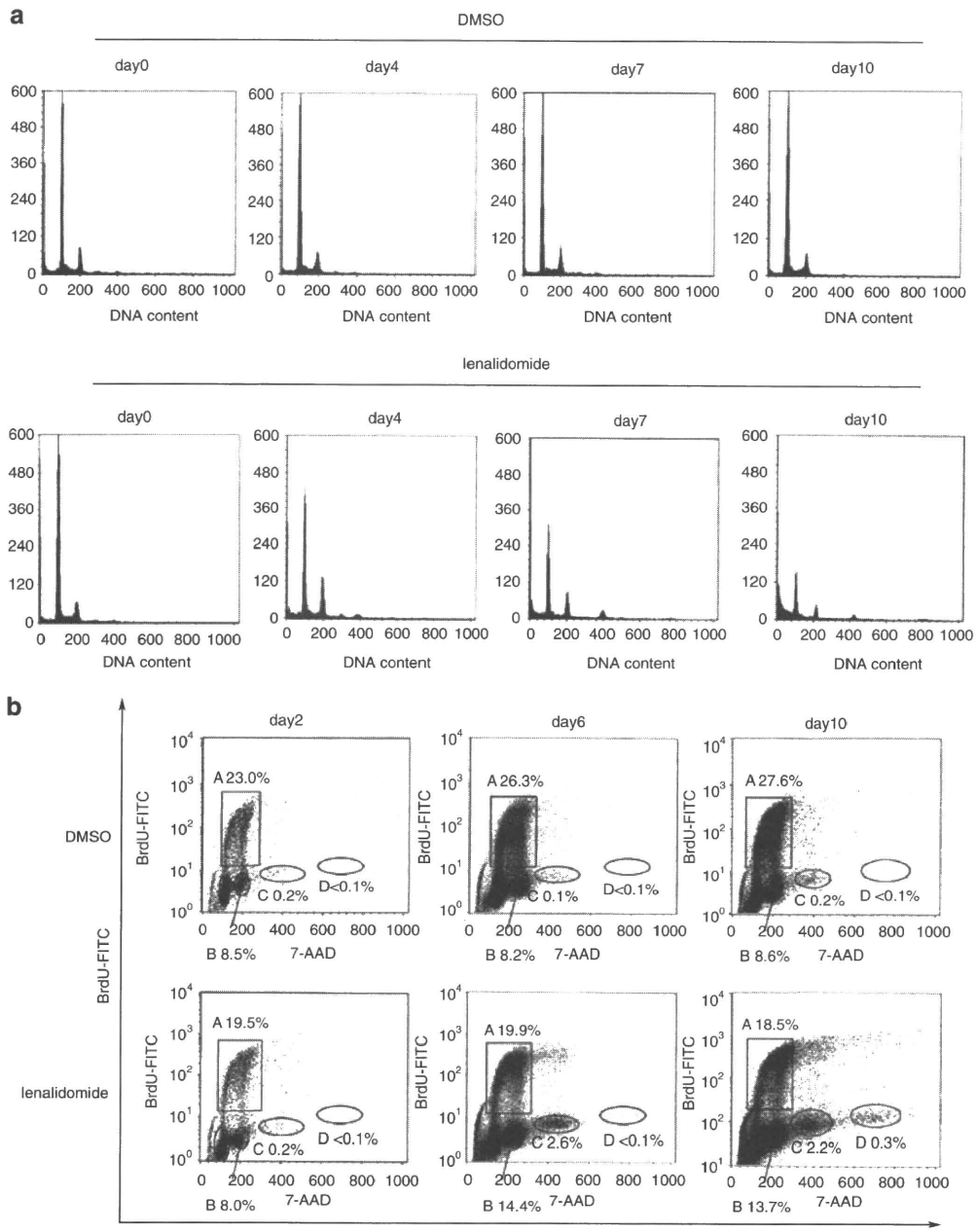

Figure 3 Lenalidomide induces the formation of polyploidy in MDS-L cells. (**a**) Cell-cycle analysis of MDS-L cells by propidium iodide (PI) staining. The cells treated with lenalidomide or DMSO for the indicated days were stained with PI for cell-cycle analysis. (**b**) Cell-cycle analysis of MDS-L cells by BrdU and 7-AAD dual staining assay. The cells treated with lenalidomide or DMSO for the indicated days were pulse-labeled for 120 min with bromodeoxyuridine (BrdU) and the incorporation of BrdU was measured together with quantification of DNA contents by 7-AAD by flow cytometry. Areas A and B indicate the fractions of ordinary diploid cells in S phase and G2/M phase, respectively. Areas C and D indicate the fractions of tetraploid and octoploid cells in G2/M phase, respectively. Ten-fold cells are plotted in the data of days 6 and 10 as compared with the data of day 2 to emphasize the presence of polyploid cells.

such as 8N and 16N were detected. Together with morphological finding, it was suggested that some parts of 4N cells entered the cell cycle again and formed hyperploid cells. The BrdU and 7-AAD dual-staining assay indicated that lenalidomide hardly inhibited DNA synthesis and a small part of the cells entered the next cell cycle from 4N to 8N to generate polyploid cells (Figure 3b). Taken together, a small part of the cells entered the next cell cycle to form multinucleated cells and finally they also died out.

Treatment with lenalidomide inhibits cytokinesis of MDS-L cells

As described above, lenalidomide treatment caused the increase in binucleated cells, but seemed not to affect DNA synthesis or mitotic division. Hence, we speculated that one of the direct action of lenalidomide is inhibition of cytokinesis. We observed lenalidomide-treated or control MDS-L cells by a time-lapse microscopy and chased the whole process of cell division. The control cells showed normal mitosis and cytokinesis and gave

rise to two daughter cells in more than 90% of observed cell division examples. In lenalidomide-treated cells, on the contrary, the cleavage furrow was formed after mitosis and the cells were about to divide into two daughter cells, but the cytokinesis was interrupted. The furrow became widened and finally binucleated cells were formed (Figure 4a). Such an aborted cytokinesis was ubiquitously detected by daily addition of lenalidomide, resulting in frequent appearance of multinucleated cells (Figure 4b, Figures 2a and b).

Treatment with lenalidomide suppresses the gene expression of M phase-related molecules in MDS-L cells

We harvested lenalidomide-treated or control MDS-L cells once on day 7 and twice on day 9, and investigated the gene expression profiling. The three independent studies represented almost the same pattern of gene expression profiles, and lenalidomide treatment resulted in the decreased gene expression of M phase-related molecules (Supplementary Table 1). Among them, the expression of *MYH10, aurora kinase B, PLK1, CDC14A* and *citron kinase* was particularly declined and these changes were also confirmed by RT–PCR (Figure 5a) and in part by immunoblotting analysis (data not shown).

As for the genes located at 5q, after lenalidomide treatment, the expression of *interferon regulatory factor 1 (IRF1)* and *KIF20A* was decreased to 0.43-fold (range: 0.34–0.49) and 0.41-fold (range: 0.05–0.65), respectively. Inversely, the expression of *early growth response 1 (EGR1), colony-stimulating factor 1*

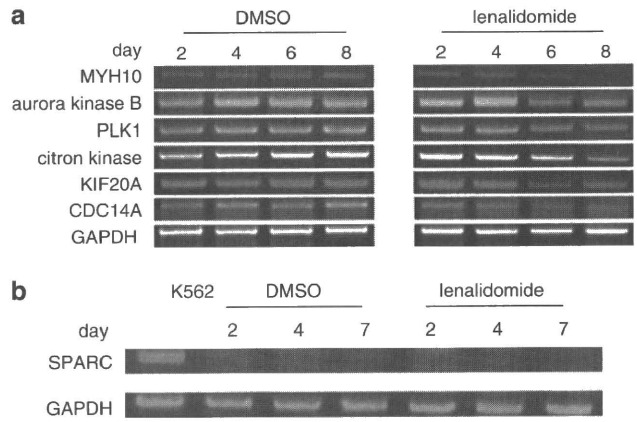

Figure 5 Lenalidomide treatment decreases the expression of M phase-related molecules. Changes in the expression of several M phase-related genes (*MYH10, aurora kinase B, PLK1, citron kinase, KIF20A, CDC14A*) (**a**) and *SPARC* (**b**) by semi quantitative RT–PCR in MDS-L cells cultured in the presence of lenalidomide or dimethylsulfoxide (DMSO) for the indicated days. K562 was used as a positive control and *GAPDH* as an internal standard.

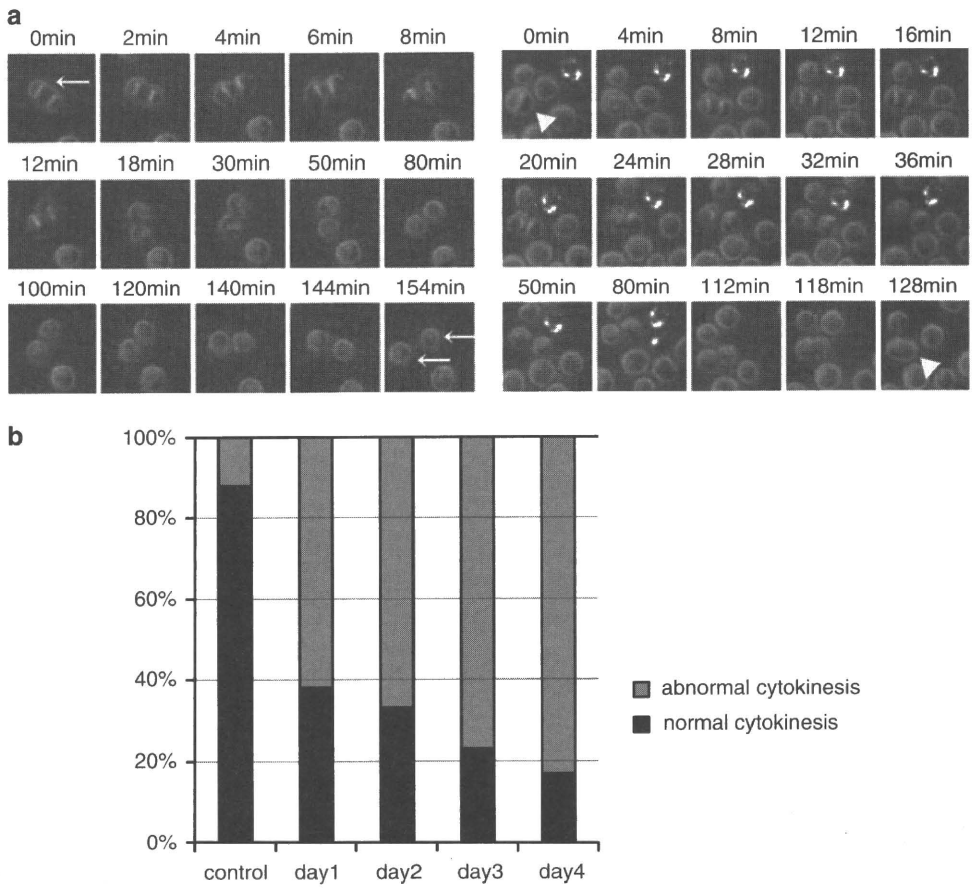

Figure 4 Lenalidomide inhibits cytokinesis of MDS-L cells. MDS-L cells were cultured for 4 days in the presence of lenalidomide or dimethylsulfoxide (DMSO) as a control, and on each day the aliquots of the cells were incubated with 100 ng/ml Hoechst 33342 for 1 h and the cell division was observed by a time-lapse microscopy. (**a**) Time-lapse images of the living cells during cell division. Arrows show a normal cell division. Arrowheads show a cell presenting abnormal cytokinesis. (**b**) The percentage of the cells presenting normal/abnormal cytokinesis was counted on the indicated days.

(*CSF-1R*) and *endothelial cell-specific molecule 2* (*ECSM2*) was increased to 11.5-fold (range: 4.7–26.5), 16.2-fold (range: 7.7–21.7) and 37.4-fold (range: 16.9–56.8), respectively. Expression of *SPARC* was rather weak or absent and not enhanced after lenalidomide treatment by RT–PCR (Figure 5b) and the gene expression profiling (data not shown).

Lenalidomide induces aberrant multiplication of centrosomes in MDS-L cells

We showed that lenalidomide induces cell death in part by formation of multinucleated cells by inhibition of cytokinesis. We also indicated that a part of polyploidy cells enter the next cell cycle (Figures 3a and b). Nigg[26] reported that the cells presenting aberrant centrosome number form multipolar spindle in the next M phase and are not able to survive because of a lack of essential genes. In fact, the mitotic cells with multiple centrosomes were observed frequently on day 4 after lenalidomide treatment in MDS-L cells (Figures 6a and b). These data suggested that aberrant multiplication of centrosomes caused by cytokinesis failure is one mechanism of lenalidomide-induced cell death.

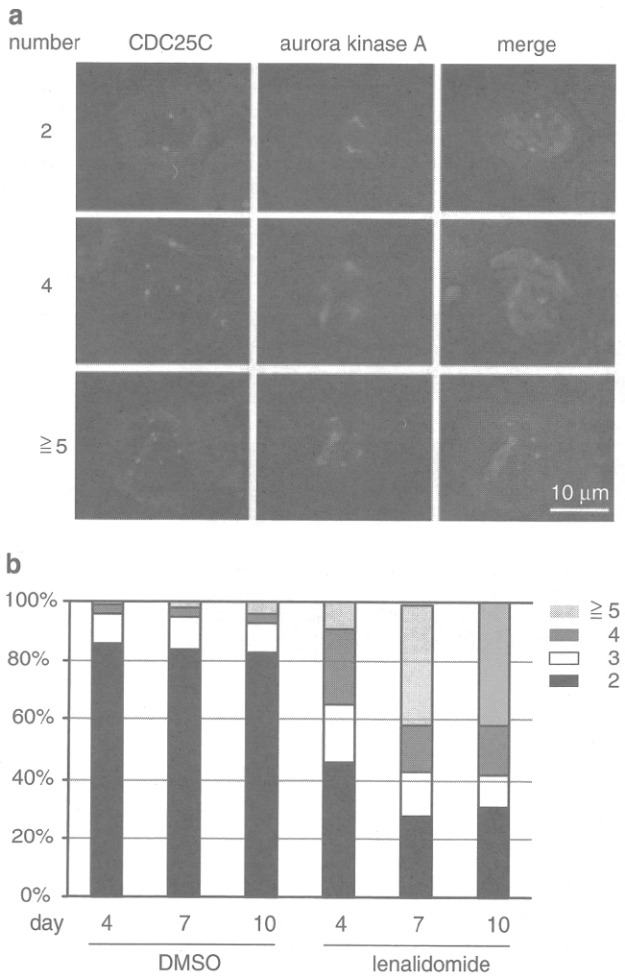

Figure 6 Lenalidomide induces aberrant multiplication of centrosomes in MDS-L cells. MDS-L cells treated with lenalidomide or dimethylsulfoxide (DMSO) were immunostained by anti-CDC25C and anti-aurora kinase A and corresponding AlexaFluor488- or AlexaFluor594-conjugated secondary antibodies. (**a**) Immunofluorescence staining of lenalidomide-treated MDS-L cells. The spots where CDC25C (green) and aurora kinase A (red) colocalized were considered as centrosomes. The chromosome area was stained with DAPI (blue) (magnification ×1000). (**b**) The number of the centrosomes in each cell (shown in percentage). More than hundred cells were examined for counting the number of centrosomes on the indicated days.

Discussion

There are important genes encoding or involved in tumor suppression, growth factors and their receptors, transcriptional factors at 5q locus, and certain genes might also be related to lenalidomide-specific growth suppression. In this study, we performed *in vitro* studies using MDS-L cell line which had been established from an MDS patient with del(5q) to further investigate del(5q)-related leukemogenesis and action mechanisms of lenalidomide.

MDS-L cell line carries a derivative small chromosome5 as a result of t(5;19)(q11;q13) and complex abnormalities instead of simple del(5q). Hence, this cell line should not be called as a typical 5q- cell line. However, an intensive study by Drexler *et al.*[22] confirmed that MDS92 (a parental cell line of MDS-L and carries the similar chromosome abnormalities including 5q change) shows the loss of BAC RP11-54C4 signal indicating 5q31-32 deletion. Therefore, MDS-L will be one of the available cell models with del(5q). Both HL-60 and KG-1 cell lines also represent del(5q) but neither of them showed growth suppression nor multinuclearity by lenalidomide treatment (data not shown). The effects of lenalidomide seem to be exerted exclusively on MDS-L cells.

Gandhi *et al.*[18] reported that lenalidomide shows an inhibitory effect on Namalwa cells by inducing G0/G1 arrest. Pellagatti *et al.*[7] reported that lenalidomide suppresses the growth of CD34-positive cells derived from the MDS with del(5q) and brings about the enhanced expression of *SPARC*. As for MDS-L, on the contrary, lenalidomide did not promote the expression of *SPARC* (Figure 5b). As one possible reason, the data by Pellagatti *et al.* seem to indicate mainly the effect on erythroid-lineage cells among the MDS progenitor cells but MDS-L cells are of the myeloid lineage and lacking in erythroid features. Another reason is that MDS-L cells carry various unknown genetic changes and might show different responses from the primary cells of 5q- syndrome to lenalidomide stimulation.

In this study, we showed that lenalidomide treatment induces multinuclearity by inhibition of cytokinesis in MDS-L cells (Figure 4). To date, several studies have indicated that the contractile ring which forms cell cleavage furrow involves various intracellular molecules: Rho-pathway molecules such as Rho GTPase, Rho kinase, citron kinase and formin; mitotic kinases, such as aurora kinase B and PLK1; molecules located on the central spindles, such as kinesin-like motors (MKLP1, MKLP2), ECT2 and MgcRacGAP.[26] Suppression of these molecules results in the formation of binucleated cells.[27,28] To approach the inhibitory mechanism of lenalidomide on cytokinesis of MDS-L cells, we inspected the gene expression profiles by microarray analysis and found decreased expression of M phase-related genes including cytokinesis-related molecules (Supplementary Table 1).

KIF20A (Rab6KIFL/MKLP2) is a kinesin-like protein, interacts with Rab6 that is associated with vesicular transport and has an important role in cytokinesis.[29,30] Interestingly, *KIF20A* is located at 5q31 and its expression was inhibited by lenalidomide treatment (Figure 5a). These results raise the possibility that *KIF20A* is one of the target genes of lenalidomide. It is also

reported that KIF20A associates with aurora kinase B and CDC14A phosphatase[31] and inhibition of *CDC14A* expression by siRNA method leads to the appearance of binucleated cells.[32] Myosin II is known to be involved in cytokinesis, and in our study the expression of *MYH10* was decreased by treatment of MDS-L with lenalidomide (Figure 5a), suggesting its relation to the inhibition of cytokinesis.

The cells which failed in cytokinesis bear multiple nuclei, and consequent multiplication of centrosomes causes impaired chromosomal segregation at the coming M phase and might result in mitotic cell death.[26,33] In fact, lenalidomide-treated MDS-L cells formed binucleated cells with four centrosomes around day 4 and then the cells with multiplicate centrosomes increased (Figure 6a). Such multinucleated cells with multiplicated centrosomes finally fall into cell death probably as a result of death induction by tetraploid checkpoint mechanism as reported by Andreassen.[34]

In our study, treatment of MDS-L cells with lenalidomide induces multinucleated cells, which are destined to die, and *KIF20A* located at 5q31 locus is proposed as a possible candidate target gene of lenalidomide. This investigation will contribute to molecular study of the myeloid malignancies with del(5q) and therapeutic mechanisms of lenalidomide. However, as MDS-L cells carry complex chromosome abnormalities besides the 5q change, the effects of lenalidomide on MDS-L might be attributable to some of the multiple genetic alterations.

The prognosis of MDS patients with del(5q) depends on various factors including additional chromosome abnormalities,[35–37] but lenalidomide exerts a favorable effect on 5q-MDS patients with complex abnormalities similarly as the patients with isolated del(5q) or to a lesser degree.[35,38,39] Our basic study might provide potentially useful issues to explain the clinical efficacy of lenalidomide on the patients with del(5q) and additional abnormalities.

Conflict of interest

K.T. has received research funding from Celgene K.K. The other authors declare no competing financial interests.

Acknowledgements

We thank Ms. Kazuko Yamane (Kawasaki Medical School) for her technical support.

This study was supported in part by the grant of the Japanese Cooperative Study Group for Intractable Bone Marrow Diseases, Ministry of Health, Labor and Welfare of Japan; in part by a Grant-in-Aid for Scientific Research from Japan Society for the Promotion of Science; and in part by Kawasaki Medical School Project Grant.

Authorship Contributions: K.T. designed the research and wrote the paper; A.M., A.T., T. N., T.K., and T.Ts. performed the experiments; M.K. performed statistical analyses; T.Ta. and Y.T. analyzed the results and contributed to useful discussion.

References

1 Heaney ML, Golde DW. Myelodysplasia. *N Engl J Med* 1999; **340**: 1649–1660.
2 Olney HJ, Le Beau MM. The cytogenetics of myelodysplastic syndromes. *Best Pract Res Clin Haematol* 2001; **14**: 479–495.
3 Van den Berghe H, Cassiman JJ, David G, Fryns JP, Michaux JL, Sokal G. Distinct haematological disorder with deletion of long arm of no. 5 chromosome. *Nature* 1974; **251**: 437–438.
4 Brunning RD, Orazi A, Germing U, Le Beau MM, Porwit A, Baumann I *et al.* Myelodysplastic syndromes. In: Swerdlow SH, *et al.* (eds). *WHO Classification of Tumours of Haematopoietic and Lymphoid Tissues.* IARC Press: Lyon, 2008, 87–107.
5 Boultwood J, Fidler C, Strickson AJ, Watkins F, Gama S, Kearney L *et al.* Narrowing and genomic annotation of the commonly deleted region of the 5q- syndrome. *Blood* 2002; **99**: 4638–4641.
6 Giagounidis AA, Germing U, Haase S, Hildebrandt B, Schlegelberger B, Schoch C *et al.* Clinical, morphological, cytogenetic, and prognostic features of patients with myelodysplastic syndromes and del(5q) including band q31. *Leukemia* 2004; **18**: 113–119.
7 Pellagatti A, Jädersten M, Forsblom AM, Cattan H, Christensson B, Emanuelsson EK *et al.* Lenalidomide inhibits the malignant clone and up-regulates the *SPARC* gene mapping to the commonly deleted region in 5q- syndrome patients. *Proc Natl Acad Sci USA* 2007; **104**: 11406–11411.
8 Liu TX, Becker MW, Jelinek J, Wu WS, Deng M, Mikhalkevich N *et al.* Chromosome 5q deletion and epigenetic suppression of the gene encoding alpha-catenin (CTNNA1) in myeloid cell transformation. *Nat Med* 2007; **13**: 78–83.
9 Joslin JM, Fernald AA, Tennant TR, Davis EM, Kogan SC, Anastasi J *et al.* Haploinsufficiency of EGR1, a candidate gene in the del(5q), leads to the development of myeloid disorders. *Blood* 2007; **110**: 719–726.
10 Ebert BL, Pretz J, Bosco J, Chang CY, Tamayo P, Galili N *et al.* Identification of RPS14 as a 5q- syndrome gene by RNA interference screen. *Nature* 2008; **451**: 335–339.
11 Wei S, Chen X, Rocha K, Epling-Burnette PK, Djeu JY, Liu Q *et al.* A critical role for phosphatase haplodeficiency in the selective suppression of deletion 5q MDS by lenalidomide. *Proc Natl Acad Sci USA* 2009; **106**: 12974–12979.
12 Dredge K, Marriott JB, Macdonald CD, Man HW, Chen R, Muller GW *et al.* Novel thalidomide analogues display anti-angiogenic activity independently of immunomodulatory effects. *Br J Cancer* 2002; **87**: 1166–1172.
13 Corral LG, Haslett PA, Muller GW, Chen R, Wong LM, Ocampo CJ *et al.* Differential cytokine modulation and T cell activation by two distinct classes of thalidomide analogues that are potent inhibitors of TNF-alpha. *J Immunol* 1999; **163**: 380–386.
14 Schafer PH, Gandhi AK, Loveland MA, Chen RS, Man HW *et al.* Schnetkamp PPEnhancement of cytokine production and AP-1 transcriptional activity in T cells by thalidomide-related immunomodulatory drugs. *J Pharmacol Exp Ther* 2003; **305**: 1222–1232.
15 Davies FE, Raje N, Hideshima T, Lentzsch S, Young G, Tai YT *et al.* Thalidomide and immunomodulatory derivatives augment natural killer cell cytotoxicity in multiple myeloma. *Blood* 2001; **98**: 210–216.
16 Muller GW, Chen R, Huang SY, Corral LG, Wong LM, Patterson RT *et al.* Amino-substituted thalidomide analogs: potent inhibitors of TNF-alpha production. *Bioorg Med Chem Lett* 1999; **9**: 1625–1630.
17 List A, Dewald G, Bennett J, Giagounidis A, Raza A, Feldman E *et al.* Lenalidomide in the myelodysplastic syndrome with chromosome 5q deletion. *N Engl J Med* 2006; **355**: 1456–1465.
18 Gandhi AK, Kang J, Naziruddin S, Parton A, Schafer PH, Stirling DI. Lenalidomide inhibits proliferation of Namalwa CSN.70 cells and interferes with Gab1 phosphorylation and adaptor protein complex assembly. *Leuk Res* 2006; **30**: 849–858.
19 Hideshima T, Chauhan D, Shima Y, Raje N, Davies FE, Tai YT *et al.* Thalidomide and its analogs overcome drug resistance of human multiple myeloma cells to conventional therapy. *Blood* 2000; **96**: 2943–2950.
20 Nakamura S, Ohnishi K, Yoshida H, Shinjo K, Takeshita A, Tohyama K *et al.* Retrovirus-mediated gene transfer of granulocyte colony-stimulating factor receptor (G-CSFR) cDNA into MDS cells and induction of their differentiation by G-CSF. *Cytokines Cell Mol Ther* 2000; **6**: 61–70.
21 Tohyama K, Tsutani H, Ueda T, Nakamura T, Yoshida Y. Establishment and characterization of a novel myeloid cell line from the bone marrow of a patient with the myelodysplastic syndrome. *Brit J Haematol* 1994; **87**: 235–242.

22 Drexler HG, Dirks WG, Macleod RA. Many are called MDS cell lines: one is chosen. *Leuk Res* 2009; **33**: 1011–1016.
23 Bonnet J, Coopman P, Morris MC. Characterization of centrosomal localization and dynamics of Cdc25C phosphatase in mitosis. *Cell Cycle* 2008; **7**: 1991–1998.
24 Tsujioka T, Tochigi A, Kishimoto M, Kondo T, Tasaka T, Wada H *et al.* DNA ploidy and cell cycle analyses in the bone marrow cells of patients with megaloblastic anemia using laser scanning cytometry. *Cytometry B Clin Cytometry* 2008; **74**: 104–109.
25 Shi Y, Tohyama Y, Kadono T, He J, Shahjahan Miah SM, Hazama R *et al.* Protein–tyrosine kinase Syk is required for pathogen engulfment in complement-mediated phagocytosis. *Blood* 2006; **107**: 4554–4562.
26 Nigg EA. Origins and consequences of centrosome aberrations in human cancers. *Int J Cancer* 2006; **119**: 2717–2723.
27 Glotzer M. The molecular requirements for cytokinesis. *Science* 2005; **307**: 1735–1739.
28 Guse A, Mishima M, Glotzer M. Phosphorylation of ZEN-4/MKLP1 by aurora B regulates completion of cytokinesis. *Curr Biol* 2005; **15**: 778–786.
29 Echard A, Jollivet F, Martinez O, Lacapère JJ, Rousselet A, Janoueix-Lerosey I *et al.* Interaction of a Golgi-associated kinesin-like protein with Rab6. *Science* 1998; **279**: 580–585.
30 Fontijn RD, Goud B, Echard A, Jollivet F, van Marle J, Pannekoek H *et al.* The human kinesin-like protein RB6K is under tight cell cycle control and is essential for cytokinesis. *Mol Cell Biol* 2001; **21**: 2944–2955.
31 Gruneberg U, Neef R, Honda R, Nigg EA, Barr FA. Relocation of Aurora B from centromeres to the central spindle at the metaphase to anaphase transition requires MKlp2. *J Cell Biol* 2004; **166**: 167–172.
32 Kaiser BK, Zimmerman ZA, Charbonneau H, Jackson PK. Disruption of centrosome structure, chromosome segregation, and cytokinesis by misexpression of human Cdc14A phosphatase. *Mol Biol Cell* 2002; **13**: 2289–2300.
33 Ganem NJ, Pellman D. Limiting the proliferation of polyploid cells. *Cell* 2007; **131**: 437–440.
34 Andreassen PR, Lohez OD, Lacroix FB, Margolis RL. Tetraploid state induces p53-dependent arrest of nontransformed mammalian cells in G1. *Mol Biol Cell* 2001; **12**: 1315–1328.
35 Giagounidis AAN, Germing U, Strupp C, Hildebrandt B, Heinsch M, Aul C. Prognosis of patients with del(5q) MDS and complex karyotype and the possible role of lenalidomide in this patient subgroup. *Ann Hematol* 2005; **84**: 569–571.
36 Tasaka T, Tohyama K, Kishimoto M, Ohyashiki K, Mitani K, Hotta T *et al.* Myelodysplastic syndrome (MDS) with chromosome 5 abnormalities: a nation-wide survey in Japan. *Leukemia* 2008; **22**: 1874–1881.
37 Kantarjian H, O'Brien S, Ravandi F, Borthakur G, Faderl S, Bueso-Ramos C *et al.* The heterogeneous prognosis of patients with myelodysplastic syndrome and chromosome 5 abnormalities: how does it relate to the original lenalidomide experience in MDS? *Cancer* 2009; **115**: 5202–5209.
38 Haferlach C, Bacher U, Tiu R, Maciejewski JP, List A. Myelodysplastic syndromes with del(5q): indications and strategies for cytogenetic testing. *Cancer Genet Cytogenet* 2008; **187**: 101–111.
39 Raza A, Reeves JA, Feldman EJ, Dewald GW, Bennett JM, Deeg HJ. Phase 2 study of lenalidomide in transfusion-dependent, low-risk, and intermediate-1 risk myelodysplastic syndromes with karyotypes other than deletion 5q. *Blood* 2008; **111**: 86–93.

Supplementary Information accompanies the paper on the Leukemia website (http://www.nature.com/leu)

Ann Hematol (2010) 89:1255–1263
DOI 10.1007/s00277-010-1020-3

ORIGINAL ARTICLE

Autoantibodies specific to hnRNP K: a new diagnostic marker for immune pathophysiology in aplastic anemia

Zhirong Qi · Hiroyuki Takamatsu · J. Luis Espinoza · Xuzhang Lu · Naomi Sugimori · Hirohito Yamazaki · Katsuya Okawa · Shinji Nakao

Received: 2 February 2010 / Accepted: 16 June 2010 / Published online: 10 July 2010

Abstract To identify a new diagnostic marker for the immune pathophysiology of aplastic anemia (AA), we screened sera of immune-mediated AA patients for the presence of antibodies (Abs) specific to proteins derived from a leukemia cell line UT-7 using two-dimensional electrophoresis followed by immunoblotting. The target proteins were identified by peptide mass fingerprinting. Heterogeneous nuclear ribonucleoprotein (hnRNP) K was identified as a novel autoantigen. An enzyme-linked immunosorbent assay revealed high titers of anti-hnRNP K Abs in 85 (31%) of 273 patients with AA. Sixty-four patients received antithymocyte globulin and cyclosporine after undergoing screening for anti-hnRNP K Ab, anti-DRS-1 Ab, anti-moesin Ab, and paroxysmal nocturnal hemoglobinuria (PNH)-type cells. Twenty (87%) of 23 patients with the presence of anti-hnRNP K Abs responded to the immunosuppressive therapy (IST), while 19 (46%) of 41 patients without the presence of anti-hnRNP K Abs responded. A multivariate analysis showed only PNH-type cells and anti-hnRNP K Abs to be significant factors for the prediction of a good response to IST. The detection of anti-hnRNP K Abs as well as PNH-type cells may therefore be useful for diagnosing the immune pathophysiology of AA.

Keywords Aplastic anemia · hnRNP K · Autoantibody · Bone marrow failure

Z. Qi · H. Takamatsu · J. L. Espinoza · X. Lu · N. Sugimori · H. Yamazaki · S. Nakao (✉)
Cellular Transplantation Biology, Kanazawa University Graduate School of Medical Science,
13-1 Takaramachi,
Kanazawa 920-8641, Japan
e-mail: snakao@med3.m.kanazawa-u.ac.jp

Z. Qi
West China Medical Center, Sichuan University,
Chengdu, China

K. Okawa
Biomolecular Characterization Unit, Frontier Technology Center,
Kyoto University Graduate School of Medicine,
Kyoto, Japan

Introduction

A large amount of laboratory and clinical data including a good response to immunosuppressive therapy (IST) suggest that the immune system attack against hematopoietic stem cells plays an essential role in the pathophysiology of aplastic anemia (AA). More than 70% of all patients with AA respond to IST with antithymocyte globulin (ATG) and cyclosporine (CsA) [1, 2]. However, IST may be detrimental to patients with non-immune-mediated AA because it potentially increases the risk of opportunistic infections and delays treatment with allogeneic stem cell transplantation. Several markers predicting good response to IST in patients with AA have been proposed. These include an increased ratio of activated T cells [3], increased interferon-γ expression in bone marrow (BM) and peripheral blood T cells [4, 5], increased expression of heat shock protein 72 [6], the presence of HLA-DRB1*1501, and small population of paroxysmal nocturnal hemoglobinuria (PNH)-type cells [7, 8]. Recent studies have demonstrated the presence of PNH-type cells to be the most reliable predictor of good response to IST [9]. However, the method for detecting small populations of PNH-type cells has not yet been generalized, possibly due to inter-lab differences in the sensitivity and the specificity of flow cytometry. PNH-type cells cannot be utilized to diagnose immune pathophysiology when fresh blood containing a sufficient number of granulocytes from patients is unavailable. Furthermore,

approximately 48% of AA patients not bearing small populations of PNH-type cells (PNH^- patients) respond to ATG and CsA therapy [8]. More reliable and universal assays that supplement the role of PNH-type cell detection are therefore required to predict a good response to IST in patients with AA.

Autoimmune diseases such as multiple sclerosis (MS) and insulin-dependent diabetes mellitus (IDDM) are characterized by the presence of autoantibodies (auto-Abs) specific to antigens derived from target organs, such as myelin basic protein in MS and glutamate decarboxylase in IDDM. These autoantibodies are detectable in the patients' sera, and the Abs serve as a marker of the immune pathophysiology of these diseases [10, 11]. Two auto-Abs specific to diazepam-binding inhibitor-related protein-1 (DRS-1) and moesin were recently identified in the sera of patients with AA. These Abs were detectable in 38% and 37% of AA patients bearing increased PNH-type cells (PNH^+ patients), but the prevalence of the Abs in PNH^- patients with AA was only 6% and 21%, respectively [12, 13]. Therefore, these Abs do not help in the diagnosis of the immune pathophysiology in PNH^- patients with AA. The identification of novel auto-Abs is therefore needed to improve the accuracy of predicting good response to IST.

This study screened sera from patients with PNH^+ AA for the presence of Abs recognizing antigens derived from a megakaryocytic leukemia cell line UT-7 using two-dimensional electrophoresis (2-DE) followed by immunoblotting and peptide mass fingerprinting.

Materials and methods

Sera and cell lines

Sera were obtained from 273 Japanese patients with AA at the time of the diagnosis. Table 1 shows characteristics of patients with AA. AA was diagnosed at Kanazawa University hospital and other hospitals taking part in the bone marrow failure (BMF) study group led by the Ministry of Health, Labor, and Welfare of Japan from December 2007 to March 2009. Sera were also obtained from 33 Japanese patients with rheumatoid arthritis (RA). Sera from 96 healthy individuals were used as controls. Samples were cryopreserved at −80°C until use. UT-7 was kindly provided by Dr N. Komatsu of Jichi Medical School. OUN-1, a cell line derived from chronic myelogenous leukemia, was kindly provided by Dr M. Yasukawa of the Ehime University. K562 and HL-60 cell lines were purchased from the Health Science Research Resource Bank (Osaka, Japan). All patients and healthy individuals provided their informed consent in accordance with the Declaration of Helsinki before sampling. This study was approved by the human research ethical committee of Kanazawa University Graduate School of Medical Science.

Table 1 Patient characteristics

Characteristics	Number	Range
Total (*n*)	273	NA
Age at diagnosis (year)	52.7	14–91
Gender (male/female)	141/132	NA
Severity (severe/moderate)	118/155	NA
Neutrophil count ($\times 10^9$/L)	830	0–2,325
Platelet count ($\times 10^9$/L)	22	2–126
Reticulocyte count ($\times 10^9$/L)	29	2–114

NA not applicable

Detection of PNH-type cells

Peripheral blood was subjected to high-sensitivity two-color flow cytometry to detect small populations of glycosylphosphatidylinositol-anchored membrane protein-deficient cells in granulocytes and erythrocytes, as described previously [8]. The presence of ≥0.003% $CD55^-CD59^-CD11b^+$ granulocytes and ≥0.005% $CD55^-CD59^-$glycophorin-A^+ erythrocytes was defined as an abnormal increase based on the results of 183 healthy individuals [9].

2-DE and western blotting

2-DE was performed as described previously with some modifications [14]. A total of 10^6 UT-7 cells were solubilized with sample preparation solution containing 7 M urea, 2 M thiourea, 4% CHAPS, 2% immobilized pH gradients (IPG) buffer pH 3–10, and 40 mM dithiothreitol (DTT; GE Healthcare, Tokyo, Japan), and the sample was diluted to 125 μl with thiourea rehydration buffer containing 7 M urea, 2 M thiourea, 2% IPG-buffer pH 3–10, 0.002% bromophenol blue, and 2.8 mg/ml DTT. Before loading into IPG-strips, the diluted sample was cleared by centrifugation (13,000 rpm for 20 min), applied to 7-cm non-linear Immobiline DryStrip of pH 3–10 (GE Healthcare) and incubated for 12 h at room temperature; then the IPG strip was subjected to first-dimensional isoelectric focusing electrophoresis (IFE) using the flatbed multiphor II electrophoresis system (GE Healthcare). The IPG strip after IFE was equilibrated twice at room temperature for 10 min with 10 ml of SDS equilibration buffer solution (6 M urea, 75 mM Tris–HCl pH 8.8, 29.3% glycerol, 2% SDS, 0.002% bromophenol blue, and 100 mg DTT or 250 mg iodoacetamide) and subjected to second dimensional SDS-PAGE. Separated proteins were transferred onto a polyvinylidene fluoride (PVDF) membrane (Millipore

Corporation, Bedford, USA) for 1.5 h at a constant current of 190 mA using a Mini Trans-Blot system (Bio-Rad, Hercules, CA) or visualized by Coomassie Brilliant Blue (CBB) staining. The blotted PVDF membranes were incubated in the presence of Tris-buffered saline (TBS) with 1% bovine serum albumin (BSA) containing serum diluted 1:200 from the patients, serum diluted 1:200 from healthy individuals or 1:2,000 diluted mouse anti-human heterogeneous nuclear ribonucleoprotein (hnRNP) K/J monoclonal Ab (mAb, clone 3C2, Sigma, USA), and then were reacted with appropriate alkaline phosphatase-labeled secondary Abs and the immunoblots were detected using a BCIP/NBT membrane alkaline phosphatase substrate system (KPL, Gaithersburg, MD, USA).

Isolation of $CD34^+$ cell

$CD34^+$ cells were isolated from the BM of healthy volunteers using a CD34 progenitor cell isolation kit (Miltenyi Biotec, Bergisch Gladbach, Germany) according to the manufacturer's instructions.

Protein identification

The proteins recognized by serum Abs were identified as previously describe [15, 16]. Briefly, after SDS-PAGE, proteins were visualized by CBB staining, and the pieces of the gel corresponding to western blotting-positive spots were excised, followed by in-gel digestions with trypsin. Molecular mass analyses of tryptic peptides were performed by matrix-assisted laser desorption/ionization time of flight mass spectrometry (MALDI-TOF MS) using an ultraflex TOF/TOF system.

Construction of the recombinant plasmid and purification of bacterially expressed protein

Full-length hnRNP K cDNA kindly provided by H. Sorimachi (Tokyo Metropolitan Organization for Medical Research) was subcloned into the pGEX-6p-1 vector (GE Healthcare) for the expression of glutathione-*S*-transferase (GST) fusion protein. Synthesized proteins were purified by glutathione sepharose 4B (GE Healthcare) according to the manufacturer's instructions. Native hnRNP K proteins were released from GST-hnRNP K fusion proteins using PreScission protease (GE Healthcare). The recombinant protein was confirmed by CBB staining and western blotting with anti-hnRNP K/J mAb.

Immunoprecipitation

Immunoprecipitation detection of anti-hnRNP K Abs using sera from patients with AA was performed according to the instructions of the Seize X Protein G Immunoprecipitation Kit (Pierce, Illinois, USA). Briefly, 10 μl of serum samples were incubated for 2 h at 4°C with 400 μl protein G-agarose beads (Pierce), and then the beads were washed three times with binding/wash buffer with centrifugation (10,000×*g* for 3 min). The beads were incubated in 200 μl of binding/wash buffer containing 1 μg of purified native hnRNP K protein for overnight at 4°C; then the beads were pelleted by centrifugation (10,000×*g* for 3 min). Thereafter, they were washed five times before the proteins were eluted from the beads with 50 μl of elution buffer for SDS-PAGE and western blotting with anti-hnRNP K/J mAb.

Determination of hnRNP K expression by hematopoietic cells

Lysates of myeloid leukemia cell lines, $CD34^+$, and peripheral blood mononuclear cells (PBMCs) from healthy individuals were obtained by suspending cell pellets in 100 μl of phosphate-buffered saline (PBS) containing protease inhibitor cocktail (Sigma Aldrich), sonicated on ice for 20 s using a B-12 Branson sonifier (Danbury, CT, USA). The cell lysates were then denatured in boiling SDS sample buffer. Equal amounts of proteins were separated by SDS-PAGE and transferred onto PVDF membrane. The membrane was incubated in 1% BSA–TBS containing 1:2,000 diluted anti-hnRNP K/J mAb or 1:5,000 diluted mouse anti-human α-tubulin mAb (clone B-5-1-2, Sigma, USA), respectively.

Enzyme-linked immunosorbent assay

Fifty microliters of coating buffer (50 mM carbonate/bicarbonate buffer, pH 9.6) containing 1 μg/ml recombinant native hnRNP K protein, recombinant native DRS-1 protein, or recombinant native moesin protein was added to each well of a 96-well Nunc-Immuno plate (Nalge-Nunc International, Roskilde, Denmark) and kept overnight at 4°C. The plates were washed and incubated with PBS containing 10% fetal bovine serum for 2 h at 37°C to block nonspecific binding. The sera from patients were added to a final dilution of 1:200 at room temperature for 2 h. After washing, the plates were incubated with 100 μl of peroxidase-conjugated goat anti-human IgG Ab (1:100,000; Jackson ImmunoResearch) at room temperature for 1 h. Finally, plates were washed and incubated with 3,3,5,5-tetramethylbenzidine substrate (Pierce, Rockford, IL) at room temperature for 30 min, and the optic density (OD) absorbance at 450 nm was read using a SLTEAR 340 ATELISA reader (SLT-Labinstruments, Grödig, Austria). A positive reaction (Ab^+) was defined as an absorbance value exceeding the mean+2 standard deviation (SD) of the OD absorbance values from the sera of the 96 healthy individuals.

Immunosuppressive therapy

Sixty-four patients with AA were treated with ATG (Lymphoglobuline, Aventis Behring, King of Prussia, PA) 15 mg/kg/day, 5 days, plus CsA (Novartis, Basel, Switzerland) 6 mg/kg/day within 1 year of diagnosis between December 2007 and March 2009. The dose of CsA was adjusted to maintain trough levels between 150 and 250 ng/ml, and the appropriate dose was administered for at least 6 months. Granulocyte colony-stimulating factor (G-CSF; filgrastim, 300 μg/m^2 or lenograstim, 5 μg/kg) was administered to some patients. The response to IST was assessed at 6 months after the IST according to the criteria proposed by Camitta [17].

Statistics

Differences in the prevalence of hnRNP K Abs among different groups were examined using a one-way analysis of variance. Correlations of anti-hnRNP K Ab titers with anti-moesin Ab titers or anti-DRS-1 Ab titers in individual patients were examined using student *t* test. The prevalence of anti-hnRNP K Abs between untransfused and transfused patients and the response rate to IST between Ab$^+$ and Ab$^-$ patients were examined using the Fisher's exact test. Logistic procedures and Fisher's exact test were used to analyze the associations between the response to IST and the prevalence of increased PNH-type cells, gender, age, severity, or three different Abs.

Results

Detection of novel auto-Abs in AA patients' sera

To detect auto-Abs specific to proteins derived from UT-7 cells, cell lysates were separated by 2-DE and subjected to western blotting using sera obtained from two PNH$^+$ untransfused patients with AA at the time of diagnosis. The sera from two patients revealed the same spot with a size of 65 kDa (Fig. 1a—ii) which was not seen on the membrane incubated with healthy individual sera (Fig. 1a—iii). The approximate isoelectric point was between 5 and 6.

Identification of the 65-kDa protein

The stained spot corresponding to the one showing positive reaction in the western blotting (Fig. 1a–i) was excised from the CBB stained gel. The proteins were eluted from the excised gel after in-gel enzyme digestion and were subjected to MALDI-TOF MS. The protein was identified as hnRNP K of which isoelectric point is 5.46. Anti-hnRNP K/J mAb revealed the same spot identified by the incubation with the patient sera (Fig. 1a—iv). Specific binding of the patients' anti-hnRNP K Abs to hnRNP K was confirmed by an immunoprecipitation analysis (Fig. 1b).

Expression of hnRNP K by hematopoietic cells

The level of expression of hnRNP K was greater in several myeloid leukemia cell lines such as HL-60, OUN-1, UT-7, and K562 than in PBMCs from healthy individuals, but there was no difference in the hnRNP K expression level between CD34$^+$ cells and PBMCs from healthy individuals (Fig. 2).

Prevalence of anti-hnRNP K Abs in patients with AA and RA

The titers of Ab specific to hnRNP K in the sera of 273 AA and 33 RA patients were determined using enzyme-linked immunosorbent assay (ELISA) with the recombinant human native hnRNP K proteins (Fig. 3a). The titers of Ab specific to hnRNP K in the sera of 273 AA and 33 RA patients were determined using ELISA with the recombinant human native hnRNP K proteins (Fig. 3a). High titers of anti-hnRNP K Abs (≥ the mean±2SD of the titers of healthy individuals, anti-hnRNP K Ab$^\pm$) were detected in 85 (31%) of the AA patients and in eight (24%) of the RA patients. There was no significant difference in the prevalence of anti-hnRNP K Abs between AA and RA patients ($P \geq 0.05$). There was no difference in the prevalence of anti-hnRNP K Abs between untransfused (27%) and transfused (33%) AA patients ($P = 0.33$). Small populations of PNH-type cells were detectable in 155 (56%) of the AA patients, and the prevalence of anti-hnRNP K Abs in PNH$^+$ and PNH$^-$ AA patients was 36% and 25%, respectively.

Correlation of anti-hnRNP K Abs with other auto-Abs

Anti-hnRNP K Ab with anti-DRS-1 Ab or anti-moesin Ab titers were measured from the same patients' sera to determine the relationship between these Abs. The anti-DRS-1 Abs and anti-moesin Abs were detectable in 29% and 28% of the 273 patients with AA, respectively. The titers of anti-hnRNP K Abs positively correlated with the presence of anti-DRS-1 Abs ($r = 0.5838$) and anti-moesin Abs ($r = 0.7239$; $P < 0.0001$; Fig. 3b).

Correlation of anti-hnRNP K Abs with response to IST

Sixty-four patients with AA of the 273 patients received ATG plus CsA therapy after the screening of three different

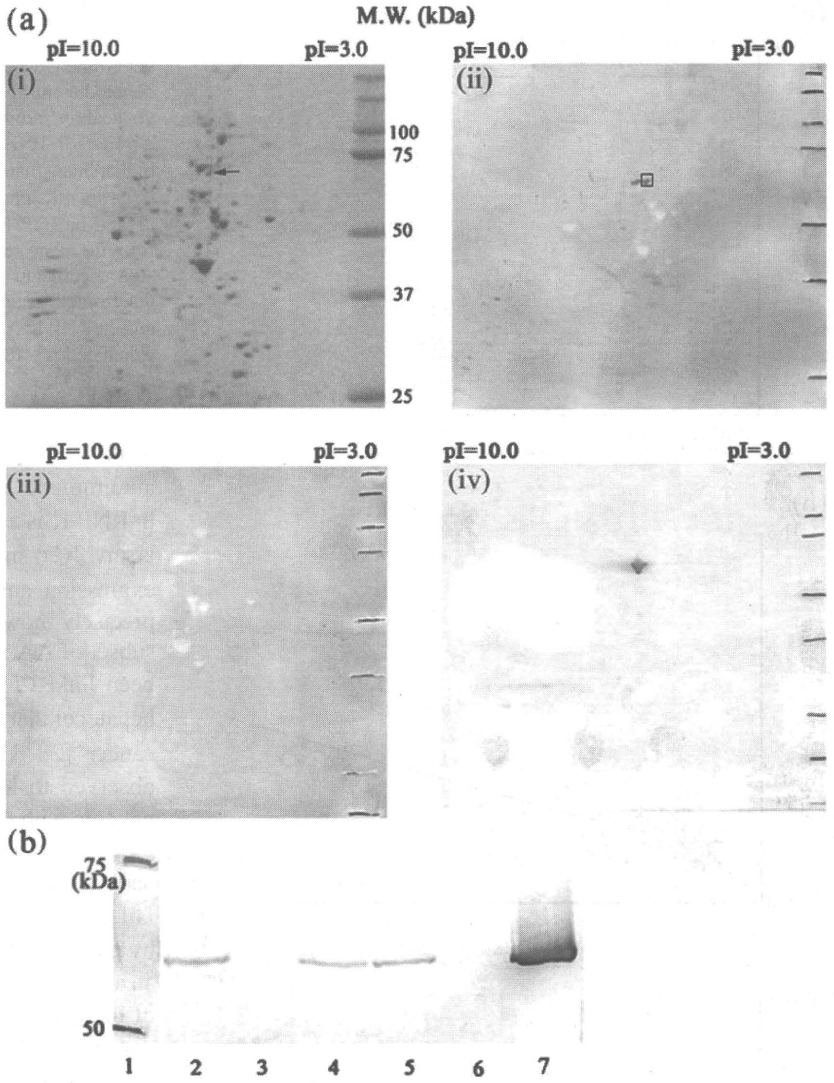

Fig. 1 Identification of the proteins derived from UT-7 cells recognized by serum Abs. **a** hnRNP K auto-Ab in serum from patient with AA. *i* UT-7 cell lysates were separated by 2-DE and visualized by CBB staining. The protein spot indicated by the *arrow* was identified as hnRNP K by mass spectrometry. *ii* UT-7 cell lysates were separated by 2-DE, transferred onto PVDF membrane, and then incubated with diluted AA patient serum (1:200). *iii* PVDF membrane was incubated with diluted healthy individual serum (1:200). *iv* PVDF membrane was incubated with diluted anti-hnRNP K/J mAb (1:2,000). **b** Immunoprecipitation detection of anti-hnRNP K Ab in the sera of patients with BMF. An equal amount of purified native hnRNP K proteins was incubated in the serum from AA patients (*lanes 2*, *4*, and *5*) and healthy individuals' sera (*lanes 3* and *6*). Anti-hnRNP K/J mAb at a 1:2,000 dilution was used as a positive control (*lane 7*)

Abs and PNH-type cells. Twenty (87%) of 23 patients with anti-hnRNP K Ab^+ responded to the IST, while 19 (46%) of 41 patients with anti-hnRNP K Ab^- responded (P=0.0015, Fig. 4a). When anti-hnRNP K Ab^+ patients were divided into two groups according to the Ab titers, there was no difference in the response rate to IST between very high titer (≥0.4, 93%) and moderately high titer (<0.4, 87%) groups (P=1.00). The response rate to IST in patients with at least one Ab^+ of three auto-Abs including anti-hnRNP K Ab, anti-DRS-1 Ab, and anti-moesin Ab was 81%, while the response rate in patients not showing Ab^+ in any of the three auto-Abs was 42% (P=0.0022; Fig. 4b). In 32 patients not displaying PNH-type cells, the response rate to IST with anti-hnRNP K Ab^+ was 86%, while only 32% patients with anti-hnRNP K Ab^- responded (P=0.0265; Fig. 4c). Multivariate analysis showed the presence of anti-hnRNP K Abs and PNH-type cells to be significant factors in the prediction of good response to IST (Table 2). Anti-hnRNP K Ab titers could be serially determined for 13 patients before and 6–7 months after IST. Four of the 13 patients showed high anti-hnRNP K Ab titers before IST. The Abs titers did not decrease either in three patients (pre-IST/post-IST: 0.3625/0.3635, 0.513/1.2455, 0.2875/0.2932) responding to IST or in one patient refractory to IST (0.413/0.318).

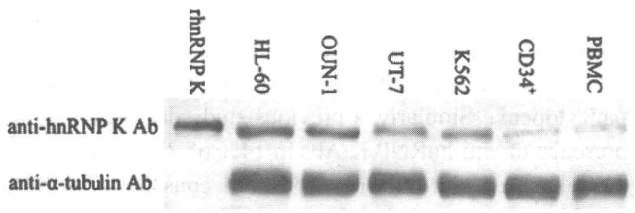

Fig. 2 Expression of hnRNP K by immature hematopoietic cells and PBMCs. An equal amount (20 μg) of cell extracts or recombinant hnRNP K protein was separated by 8% SDS-PAGE, transferred to PVDF membrane, and reacted with anti-hnRNP K/J mAb at a 1:2,000 dilution or anti-α-tubulin mAb at a 1:5,000 dilution

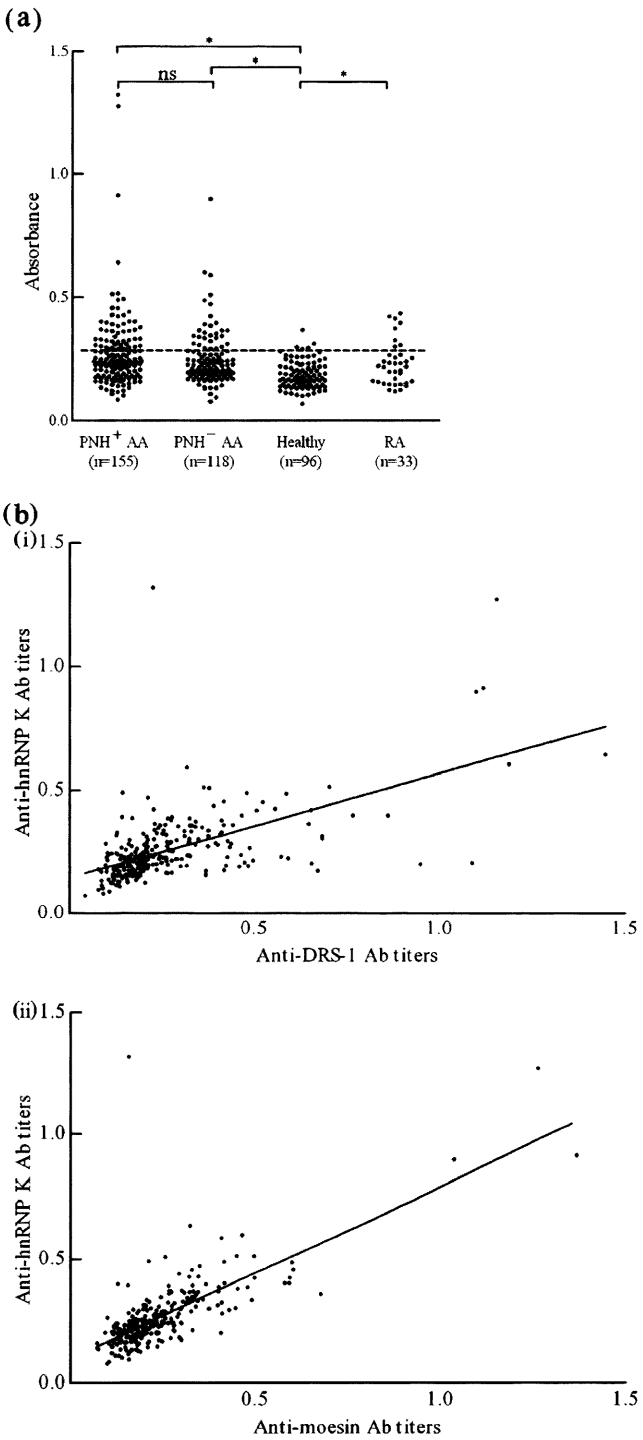

◀ **Fig. 3** Titration of anti-hnRNP K Abs in patients' sera using ELISA. **a** Antibody titers against purified hnRNP K proteins in the sera were determined using diluted sera at a 1:200 dilution. The *dotted line* denoted a cutoff value defined as the mean+2SD of the absorbance in 96 healthy individuals. *Asterisks* indicate a prevalence of hnRNP K Ab titers in PNH^+ AA, PNH^- AA, and RA patients' sera significantly higher than that of hnRNP K Ab titers in healthy individuals (*$P<0.05$; *ns* no significant meaning). **b** The correlation between the titers of anti-hnRNP K Ab and either anti-DRS-1 Ab or anti-moesin Ab from the same sera obtained from AA patients was examined. Titers of Abs specific to native hnRNP K, DRS-1, and moesin protein were determined using diluted sera at a 1:200 dilution, and correlations of anti-hnRNP K Ab titers with each of other two Ab titers (*i* and *ii*) were calculated ($P<0.0001$)

Discussion

The present study identified anti-hnRNP K Abs as a novel auto-Ab in the serum of patients with immune-mediated AA. hnRNPs are among the most abundant proteins in the eukaryotic cell nucleus and play a direct role in several aspects of RNA activity including splicing, export of the mature RNAs, and translation. Approximately 30 hnRNPs have been identified [18]. More and more evidence points to hnRNPs as important intracellular target antigens of the autoimmune response in autoimmune diseases [19–25]. hnRNP K is a conserved RNA/DNA-binding protein which is involved in the multiple steps that comprise both gene expression and signal transduction [26, 27]. It is unclear precisely how the anti-hnRNP K Abs were raised in a subset of AA patients. The overexpression of hnRNP K has been linked to a range of cancers including breast cancer, hepatocellular carcinoma, esophageal cancer, and colorectal cancer [28–31]. The hnRNP K protein expression was observed to increase in the $CD34^+$ bone marrow cells of patients with CML in the accelerated and blastic phase, but it did not increase in the $CD34^+$ cells of chronic phase CML patients and of healthy donors [32]. The present study failed to detect an increased expression of hnRNP K protein by $CD34^+$ cells from healthy individuals as well. However, an increased expression of hnRNP K was detectable in all of the examined myeloid leukemia cell lines. It is therefore possible that the destruction of immature hematopoietic cells that express high levels of hnRNP K may induce a specific immune response to hnRNP K in patients with immune-mediated AA.

The ELISA detected significantly higher titers of anti-hnRNP K Abs in comparison to healthy controls in 56 (36%) of 155 patients with immune-mediated AA displaying increased PNH-type cells and in 29 (25%) of 118 patients without increased PNH-type cells in the current study, and there was no significant difference in the prevalence of anti-hnRNP K Abs between these two groups. High titers of anti-hnRNP K Abs were also detected in 24% of RA patients not showing apparent signs of pancytopenia. Similarly, a previous study demonstrated the presence of anti-hnRNP K Abs in 14% of RA patients [33]. Therefore, anti-hnRNP K Ab is not considered to be a specific marker for the presence of the immune attack against hematologic stem cells. However, a case–control study on AA conducted by the International Agranulocytosis and AA Study revealed that a past history of RA is significantly associated with the subsequent development of AA [34], and previous studies revealed the presence of anti-

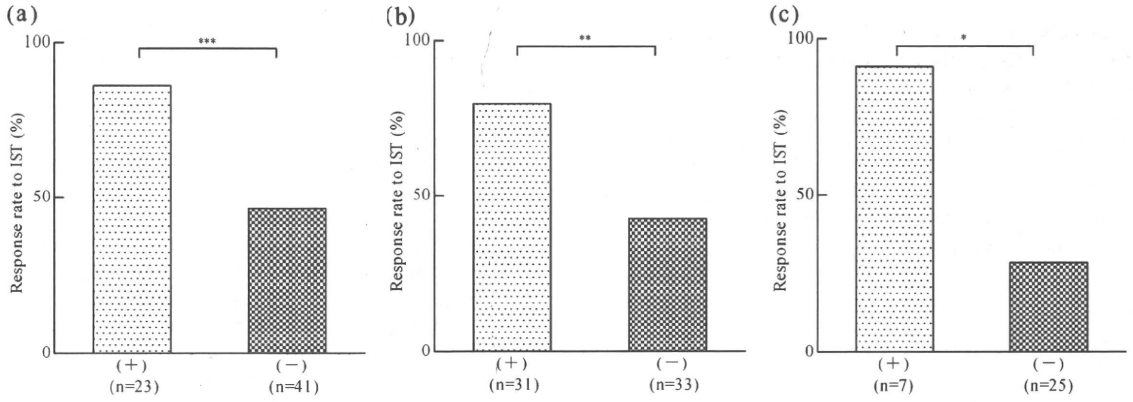

Fig. 4 The relationships between anti-hnRNP K Abs and response rate to IST in patients with BMF. The response rates to IST were compared between the following patient groups. **a** Patients with anti-hnRNP K Abs (+) and those without anti-hnRNP K Abs (−). **b** Patients showing at least one Ab^+ of three auto-Abs (+) and patients not showing Ab^+ in any of the three auto-Abs (–). **c** PNH^- patients with anti-hnRNP K Ab^+ (+) and those anti-hnRNP K Ab^- (–) (***P=0.0015, **P=0.0022, *P=0.0265)

moesin Abs in 14% of patients with RA and in 37% of patients with AA [13, 35]. These findings suggest that AA and RA may share pathogenetic mechanisms characterized by a breakdown of immune tolerance to moesin and hnRNP K. It remains unclear why bone marrow failure develops only in AA despite the sharing of immune mechanisms. Although a breakdown of immune tolerance toward multiple autoantigens occurs in both diseases, the breakdown toward antigens on hematopoietic stem cells may occur only in patients with AA.

A strong correlation was found between the presence of anti-hnRNP K Abs and that of anti-DRS-1 Abs or anti-moesin Abs in patients with AA in the present study, indicating that a propensity of patients with immune-mediated AA thus undergo a breakdown of immune tolerance toward multiple autoantigens, possibly including pathogenic autoantigens in AA. Therefore, anti-hnRNP K Abs may serve as an indirect marker for the presence of immune pathophysiology of AA. Indeed, the presence of anti-hnRNP K Abs predicted a response to IST either by itself or in combination with anti-DRS-1 Abs or anti-moesin Abs, even in PNH^- patients with AA (Fig. 4). Among the three different Abs, only the presence of anti-hnRNP K Abs proved to be a significant factor for a good response to IST based on a multivariate analysis. Therefore, the detection of anti-hnRNP K Abs alone or together with anti-DRS-1 Abs and anti-moesin Abs may be useful in choosing the optimal therapy for AA patients, particularly when PNH-type cell detection is inapplicable. Recent reports showed that some patients with AA improved with anti-CD20 Ab (rituximab) therapy [36, 37]. The detection of these auto-Abs may also be useful for identifying AA patients who are likely to respond to such anti-CD20 Ab therapy.

Fritsch et al. [38] recently reported that hnRNP A2-specific T cell clones from patients with RA show a strong Th1 phenotype and secrete higher amounts of IFN-γ than Th1 clones from controls. Inhibition experiments performed with mAb specific to MHC class II molecules show that the hnRNP A2-induced T cell responses are largely HLA-DR restricted. $CD4^+$ T cells play an important role in the development of AA as well as of HLA-DRB1*1501 [9, 12]. Specific immune responses to hnRNP K may induce the polarization of Th1 $CD4^+$ cells and may thereby contribute to development of AA. Identification of hnRNP K-specific T cells with HLA class II tetramers and a functional analysis of those would help further clarify the roles of immune response specific to hnRNP K in the pathophysiology of AA.

Table 2 Pretreatment variables associated with a response to ATG plus CsA therapy

Favorable factors	*P* value	
	Univariate[a]	Multivariate[b]
Gender (male vs. female)	1.0000	0.8770
Age (at least 40 years vs. younger)	1.0000	0.4380
Severity (severe vs. moderate)	0.5085	0.8540
PNH-type cell (positive vs. negative)	0.0097	0.0370
Anti-DRS-1 Abs (positive vs. negative)	0.5610	0.7800
Anti-moesin Abs (positive vs. negative)	0.0036	0.5800
Anti-hnRNP K Abs (positive vs. negative)	0.0004	0.0120

[a] Fisher's exact probability test

[b] Wald c^2 test for a logistic regression model

Acknowledgments The authors would like to thank R. Oumi and T. Tanaka of Cellular Transplantation Biology of Kanazawa University who provided some technical assistance and all of the BMF study groups who provided sera of patients to this study. This work was supported by a grant from Grant-in-Aid for Scientific Research from the Ministry of Education, Science, Technology, Sports and Culture of Japan (KAKENHI No. 21390291) and grants from the Research Committee for Idiopathic Hematopoietic Disorders, the Ministry of Health, Labor, and Welfare, Japan.

References

1. Rosenfeld SJ, Kimball J, Vining D, Young NS (1995) Intensive immunosuppression with antithymocyte globulin and cyclosporine as treatment for severe acquired aplastic anemia. Blood 85 (11):3058–3065
2. Bacigalupo A, Broccia G, Corda G, Arcese W, Carotenuto M, Gallamini A, Locatelli F, Mori PG, Saracco P, Todeschini G, Coser P, Iacopino P, Vanlint MT, Gluckman E (1995) Antilymphocyte globulin, cyclosporin, and granulocyte colony-stimulating factor in patients with acquired severe aplastic anemia (SAA): a pilot study of the EBMT SAA Working Party. Blood 85(5):1348–1353
3. Maciejewski JP, Hibbs JR, Anderson S, Katevas P, Young NS (1994) Bone marrow and peripheral blood lymphocyte phenotype in patients with bone marrow failure. Exp Hematol 22(11):1102–1110
4. Nakao S, Yamaguchi M, Shiobara S, Yokoi T, Miyawaki T, Taniguchi T, Matsuda T (1992) Interferon-gamma gene expression in unstimulated bone marrow mononuclear cells predicts a good response to cyclosporine therapy in aplastic anemia. Blood 79 (10):2532–2535
5. Sloand E, Kim S, Maciejewski JP, Tisdale J, Follmann D, Young NS (2002) Intracellular interferon-gamma in circulating and marrow T cells detected by flow cytometry and the response to immunosuppressive therapy in patients with aplastic anemia. Blood 100(4):1185–1191
6. Takami A, Nakao S, Tatsumi Y, Wang HB, Zeng WH, Yamazaki H, Yasue S, Shiobara S, Matsuda T, Mizoguchi H (1999) High inducibility of heat shock protein 72 (hsp72) in peripheral blood mononuclear cells of aplastic anaemia patients: a reliable marker of immune-mediated aplastic anaemia responsive to cyclosporine therapy. Br J Haematol 106(2):377–384
7. Nakao S, Takamatsu H, Chuhjo T, Ueda M, Shiobara S, Matsuda T, Kaneshige T, Mizoguchi H (1994) Identification of a specific HLA class II haplotype strongly associated with susceptibility to cyclosporine-dependent aplastic anemia. Blood 84(12):4257–4261
8. Sugimori C, Chuhjo T, Feng XM, Yamazaki H, Takami A, Teramura M, Mizoguchi H, Omine M, Nakao S (2006) Minor population of CD55(-)CD59(-) blood cells predicts response to immunosuppressive therapy and prognosis in patients with aplastic anemia. Blood 107(4):1308–1314. doi:10.1182/blood-2005-06-2485
9. Sugimori C, Yamazaki H, Feng XM, Mochizuki K, Kondo Y, Takami A, Chuhjo T, Kimura A, Teramura M, Mizoguchi H, Omine M, Nakao S (2007) Roles of DRB1*1501 and DRB1*1502 in the pathogenesis of aplastic anemia. Exp Hematol 35(1):13–20. doi:10.1016/j.exphem.2006.09.002
10. Berger T, Rubner P, Schautzer F, Egg R, Ulmer H, Mayringer I, Dilitz E, Deisenhammer F, Reindl M (2003) Antimyelin antibodies as a predictor of clinically definite multiple sclerosis after a first demyelinating event. N Engl J Med 349(2):139–145
11. Ronkainen MS, Harkonen T, Perheentupa J, Knip M (2005) Characterization of the humoral immune response to glutamic acid decarboxylase in patients with autoimmune polyendocrinopathy-candidiasis-ectodermal dystrophy (APECED) and/or type 1 diabetes. Eur J Endocrinol 153(6):901–906. doi:10.1530/eje.1.02026
12. Feng XM, Chuhjo T, Sugimori C, Kotani T, Lu XZ, Takami A, Takamatsu H, Yamazaki H, Nakao S (2004) Diazepam-binding inhibitor-related protein 1: a candidate autoantigen in acquired aplastic anemia patients harboring a minor population of paroxysmal nocturnal hemoglobinuria-type cells. Blood 104(8):2425–2431. doi:10.1182/blood-2004-05-1839
13. Takamatsu H, Feng XM, Chuhjo T, Lu XZ, Sugimori C, Okawa K, Yamamoto M, Iseki S, Nakao S (2007) Specific antibodies to moesin, a membrane-cytoskeleton linker protein, are frequently detected in patients with acquired aplastic anemia. Blood 109 (6):2514–2520. doi:10.1182/blood-2006-07-036715
14. Nyman TA, Rosengren A, Syyrakki S, Pellinen TP, Rautajoki K, Lahesmaa R (2001) A proteome database of human primary T helper cells. Electrophoresis 22(20):4375–4382
15. Jensen ON, Podtelejnikov A, Mann M (1996) Delayed extraction improves specificity in database searches by matrix-assisted laser desorption/ionization peptide maps. Rapid Commun Mass Spectrom 10(11):1371–1378
16. Yates JR (1998) Mass spectrometry and the age of the proteome. J Mass Spectrom 33(1):1–19
17. Camitta BM (2000) What is the definition of cure for aplastic anemia? Acta Haematol 103(1):16–18
18. Caporali R, Bugatti S, Bruschi E, Cavagna L, Montecucco C (2005) Autoantibodies to heterogeneous nuclear ribonucleoproteins. Autoimmunity 38(1):25–32. doi:10.1080/08916930400022590
19. Hassfeld W, Steiner G, Hartmuth K, Kolarz G, Scherak O, Graninger W, Thumb N, Smolen JS (1989) Demonstration of a new antinuclear antibody (anti-RA33) that is highly specific for rheumatoid arthritis. Arthritis Rheum 32(12):1515–1520
20. GA DA, Vretou E, Sekeris CE (1988) Autoantibodies to the core proteins of hnRNPs. FEBS Lett 231(1):118–124
21. KE JL, Wilson SH, Steinberg AD, Klinman DM (1988) Antibodies from patients and mice with autoimmune diseases react with recombinant hnRNP core protein A1. J Autoimmun 1(1):73–83
22. Montecucco C, Caporali R, Negri C, de Gennaro F, Cerino A, Bestagno M, Cobianchi F, Astaldi-Ricotti GC (1990) Antibodies from patients with rheumatoid arthritis and systemic lupus erythematosus recognize different epitopes of a single heterogeneous nuclear RNP core protein. Possible role of cross-reacting antikeratin antibodies. Arthritis Rheum 33(2):180–186
23. Steiner G, Hartmuth K, Skriner K, Maurerfogy I, Sinski A, Thalmann E, Hassfeld W, Barta A, Smolen JS (1992) Purification and partial sequencing of the nuclear autoantigen RA33 shows that it is indistinguishable from the A2 protein of the heterogeneous nuclear ribonucleoprotein complex. J Clin Investig 90(3):1061–1066
24. Hassfeld W, Steiner G, Studnickabenke A, Skriner K, Graninger W, Fischer I, Smolen JS (1995) Autoimmune response to the spliceosome. An immunologic link between rheumatoid arthritis, mixed connective tissue disease, and systemic lupus erythematosus. Arthritis Rheum 38(6):777–785
25. Jones DA, Yawalkar N, Suh KY, Sadat S, Rich B, Kupper TS (2004) Identification of autoantigens in psoriatic plaques using expression cloning. J Investig Dermatol 123(1):93–100. doi:10.1111/j.0022-202X.2004.22709.x
26. Bomsztyk K, VanSeuningen I, Suzuki H, Denisenko O, Ostrowski J (1997) Diverse molecular interactions of the hnRNP K protein. FEBS Lett 403(2):113–115
27. Bomsztyk K, Denisenko O, Ostrowski J (2004) HnRNP K: One protein multiple processes. Bioessays 26(6):629–638. doi:10.1002/bies.20048
28. Mandal M, Vadlamudi R, Nguyen D, Wang RA, Costa L, Bagheri-Yarmand R, Mendelsohn J, Kumar R (2001) Growth factors regulate heterogeneous nuclear ribonucleoprotein K expression and function. J Biol Chem 276(13):9699–9704

29. Li C, Hong Y, Tan YX, Zhou H, Ai JH, Li SJ, Zhang L, Xia QC, Wu JR, Wang HY, Zeng R (2004) Accurate qualitative and quantitative proteomic analysis of clinical hepatocellular carcinoma using laser capture microdissection coupled with isotope-coded affinity tag and two-dimensional liquid chromatography mass spectrometry. Mol Cell Proteomics 3(4):399–409. doi:10.1074/mcp.M300133-MCP200
30. Hatakeyama H, Kondo T, Fujii K, Nakanishi Y, Kato H, Fukuda S, Hirohashi S (2006) Protein clusters associated with carcinogenesis, histological differentiation and nodal metastasis in esophageal cancer. Proteomics 6(23):6300–6316. doi:10.1002/pmic.200600488
31. Klimek-Tomczak K, Mikula M, Dzwonek A, Paziewska A, Karczmarski J, Hennig E, Bujnicki JM, Bragoszewski P, Denisenko O, Bomsztyk K, Ostrowski J (2006) Editing of hnRNP K protein mRNA in colorectal adenocarcinoma and surrounding mucosa. Br J Cancer 94(4):586–592. doi:10.1038/sj.bjc.6602938
32. Notari M, Neviani P, Santhanam R, Blaser BW, Chang JS, Galietta A, Willis AE, Roy DC, Caligiuri MA, Marcucci G, Perrotti D (2006) A MAPK/HNRPK pathway controls BCR/ABL oncogenic potential by regulating MYC mRNA translation. Blood 107(6):2507–2516. doi:10.1182/blood-2005.09.3732
33. Valai A, Belisova A, Hayer S, Hoefler E, Steiner G (2004) The RNA binding domains of hnRNP K contain major autoepitopes targeted by patients with SLE and other autoimmune diseases. In: ICI/FOCISed. Abstract number 1148
34. Kaufman DW, Kelly JP, Levy M, Shapiro S (eds) (1991) The drug etiology of agranulocytosis and aplastic anemia: the international agranulocytosis and aplastic anemia study. Oxford University Press, New York
35. Wagatsuma M, Kimura M, Suzuki R, Takeuchi F, Matsuta K, Watanabe H (1996) Ezrin, radixin and moesin are possible autoimmune antigens in rheumatoid arthritis. Mol Immunol 33 (15):1171–1176
36. Hansen PB, Lauritzen AMF (2005) Aplastic anemia successfully treated with rituximab. Am J Hematol 80(4):292–294. doi:10.1002/ajh.20428
37. Castiglioni MG, Scatena P, Pandolfo C, Mechelli S, Bianchi M (2006) Rituximab therapy of severe aplastic anemia induced by fludarabine and cyclophosphamide in a patient affected by B-cell chronic lymphocytic leukemia. Leuk Lymphoma 47(9):1985–1986. doi:10.1080/10428190600709630
38. Fritsch R, Eselbock D, Skriner K, Jahn-Schmid B, Scheinecker C, Bohle B, Tohidast-Akrad M, Hayer S, Neumuller J, Pinol-Roma S, Smolen JS, Steiner G (2002) Characterization of autoreactive T cells to the autoantigens heterogeneous nuclear ribonucleoprotein A2 (RA33) and filaggrin in patients with rheumatoid arthritis. J Immunol 169(2):1068–1076

VOLUME 29 · NUMBER 4 · FEBRUARY 1 2011

JOURNAL OF CLINICAL ONCOLOGY ORIGINAL REPORT

Risk of Myelodysplastic Syndromes in People Exposed to Ionizing Radiation: A Retrospective Cohort Study of Nagasaki Atomic Bomb Survivors

Masako Iwanaga, Wan-Ling Hsu, Midori Soda, Yumi Takasaki, Masayuki Tawara, Tatsuro Joh, Tatsuhiko Amenomori, Masaomi Yamamura, Yoshiharu Yoshida, Takashi Koba, Yasushi Miyazaki, Tatsuki Matsuo, Dale L. Preston, Akihiko Suyama, Kazunori Kodama, and Masao Tomonaga

From the Atomic Bomb Disease Institute, Nagasaki University Graduate School of Biomedical Science; Kwassui Women's College; Radiation Effects Research Foundation; Japanese Red Cross Nagasaki Genbaku Hospital; St. Francis Hospital; Nagasaki Municipal Hospital; Nagasaki Atomic Bomb Casualty Council Health Management Center; and Nagasaki Municipal Medical Center, Nagasaki; Radiation Effects Research Foundation, Hiroshima, Japan; and Hirosoft International, Seattle, WA.

Submitted June 28, 2010; accepted October 15, 2010; published online ahead of print at www.jco.org on December 13, 2010.

Supported by Grants No. 17590545 and 20590649 and in part by the 21st Century Research Centers of Excellence Radiation Medical Program Grant No. 17301, E-17 to Nagasaki University, all from the Ministry of Education, Culture, Sports, Science and Technology of Japan, and by the Japanese Ministry of Health, Labor, and Welfare and the US Department of Energy, with funding provided in part through the National Academy of Sciences to the Radiation Effects Research Foundation.

Presented as an oral presentation at the International Myelodysplastic Syndromes Symposium, May 12, 2005, Nagasaki, Japan, and at the International Symposium of the 21st Century Research Centers of Excellence Radiation Medical Program Grant, March 8, 2005, Nagasaki, Japan.

Authors' disclosures of potential conflicts of interest and author contributions are found at the end of this article.

Corresponding author: Masako Iwanaga, MD, MPH, Department of Hematology and Molecular Medicine, Atomic Bomb Disease Institute, Nagasaki University Graduate School of Biomedical Sciences, 1-12-4 Sakamoto, Nagasaki, 852-8523, Japan; e-mail: masakoiwng@gmail.com.

0732-183X/11/2904-428/$20.00

DOI: 10.1200/JCO.2010.31.3080

ABSTRACT

Purpose
The risk of myelodysplastic syndromes (MDS) has not been fully investigated among people exposed to ionizing radiation. We investigate MDS risk and radiation dose-response in Japanese atomic bomb survivors.

Patients and Methods
We conducted a retrospective cohort study by using two databases of Nagasaki atomic bomb survivors: 64,026 people with known exposure distance in the database of Nagasaki University Atomic-Bomb Disease Institute (ABDI) and 22,245 people with estimated radiation dose in the Radiation Effects Research Foundation Life Span Study (LSS). Patients with MDS diagnosed from 1985 to 2004 were identified by record linkage between the cohorts and the Nagasaki Prefecture Cancer Registry. Cox and Poisson regression models were used to estimate relationships between exposure distance or dose and MDS risk.

Results
There were 151 patients with MDS in the ABDI cohort and 47 patients with MDS in the LSS cohort. MDS rate increased inversely with exposure distance, with an excess relative risk (ERR) decay per km of 1.2 (95% CI, 0.4 to 3.0; $P < .001$) for ABDI. MDS risk also showed a significant linear response to exposure dose level ($P < .001$) with an ERR per Gy of 4.3 (95% CI, 1.6 to 9.5; $P < .001$). After adjustment for sex, attained age, and birth year, the MDS risk was significantly greater in those exposed when young.

Conclusion
A significant linear radiation dose-response for MDS exists in atomic bomb survivors 40 to 60 years after radiation exposure. Clinicians should perform careful long-term follow-up of irradiated people to detect MDS as early as possible.

J Clin Oncol 29:428-434. © 2010 by American Society of Clinical Oncology

INTRODUCTION

Myelodysplastic syndromes (MDS) are a heterogeneous group of disorders characterized by clonal and ineffective hematopoiesis, morphologic dysplasia, and an increased risk of developing acute myeloid leukemia (AML).[1] MDS can arise de novo or secondary after chemo- and/or radiotherapy (therapy-related MDS).

The pathogenesis and established causative factors remain elusive for most patients with MDS. A widely accepted multistep pathogenesis model involves initial damage to hematopoietic stem cells caused by genotoxic or environmental agents followed by additional genetic or cytogenetic changes, resulting in the expansion of the MDS clone and the subsequent leukemic transformation.[2,3] Ionizing radiation is a well-known environmental carcinogen that induces chromosomal and genetic abnormalities. When an individual's bone marrow is exposed to ionizing radiation, hematopoietic stem cells may be damaged randomly, and some of these changes could induce MDS.

In contrast to the well-documented radiation-induced leukemia,[4-6] there has been no conclusive evidence that radiation exposure plays a significant role in the development of MDS. So far, radiation exposure remains a probable causative factor for MDS.[2] Most review articles have described radiation exposure as a definite causative factor for MDS on the basis of clinical studies of therapy-related MDS/AML. However, the original sources seldom

evaluated the radiation dose-response relationship for MDS alone. Epidemiologic studies of people exposed to a variety of radiations reported only a small number of cases.[7-10] In a previous study of atomic bomb survivors,[11] a possible radiation dose-response relationship for MDS was suggested, but the analysis included only 12 patients. MDS research among the atomic bomb survivors has been hampered by the fact that case ascertainment was incomplete before publication of the 1982 French-American-British (FAB) classification[1] and that no regional cancer registry officially registered MDS until 2000.

A radiation dose-response relationship for MDS might be predictable from that for AML because of the clinical similarity between the two diseases. However, much data have been accumulated to support that MDS has features that are distinct from AML with regard to latency of onset, genetic and cytogenetic abnormalities, apoptotic activity, and so on.[12,13] These biologic differences between MDS and AML suggest that radiation-induced MDS and AML may have distinct features as a consequence of different damage caused by radiation exposure. Therefore, it is important to evaluate the radiation dose relationship for MDS risk in people exposed to radiation.

In response to the increasing concern about MDS risk in atomic bomb survivors,[14] we initiated a multi-institutional epidemiologic research project. The aim of this study was to assess MDS risk and the radiation dose-response relationship 40 to 60 years after exposure.

PATIENTS AND METHODS

Study Project

This project, begun in April 2004, was a collaboration between the Atomic Bomb Disease Institute (ABDI) of the Nagasaki University Graduate School of Biomedical Sciences, the Nagasaki Prefecture Cancer Registry (NPCR),[15] the hematology departments in five hospitals in Nagasaki City (see Acknowledgment), and the Radiation Effects Research Foundation (RERF). The Institutional Review Boards of Nagasaki University (Research Protocol 16031797) and RERF (Research Protocols 18-66 and 1-75) approved this study.

Patients

We collected clinical information on MDS patients diagnosed in the five hospitals from 1982 to 2004, without regard for exposure status. Skilled hematologists in the hospitals and two authors (M.I. and M.To.) re-evaluated the clinical information, including bone marrow specimens, by using FAB criteria[1] to classify patients as refractory anemia (RA), RA with ringed sideroblasts (RARS), RA with excess blasts (RAEB), RAEB in transformation (RAEB-t), or chronic myelomonocytic leukemia (CMML). We also classified the diagnostic certainty for each patient as either definite, possible, undetermined, or non-MDS by using the criteria listed in Table 1. All reviewed patients were reported to the NPCR to be checked for multiple enrollments, the earliest date of MDS diagnosis, and the presence of malignancies before the MDS diagnosis. MDS patients who received chemotherapy and/or radiation therapy for their earlier malignancy were treated as therapy-related MDS, but those who had only surgery for their earlier malignancy were treated as primary MDS. International Classification of Diseases for Oncology, 3rd Edition (ICD-O-3) codes[16] for MDS were assigned to all patients. We also added information on date of death, date of progression to overt leukemia, if present, and the last recorded follow-up date.

Population

We used two different cohorts of Nagasaki atomic bomb survivors: a cohort defined by the ABDI Data Center and RERF's Life Span Study (LSS) cohort. Although there is some overlap between the cohorts, they were established independently and each has its own strengths and limitations. The ABDI cohort is larger than the LSS cohort but lacks information on individual dose, whereas the LSS cohort has detailed individual dose estimates but fewer Nagasaki survivors. The main reason for using two cohorts in our study was to give more credibility to the LSS dose-response findings by confirming similar distance-response patterns in the two cohorts.

The ABDI database was established in 1977 and consists of data on approximately 120,000 Nagasaki atomic bomb survivors. Available data include information on exposure status, death and migration dates, and the results of medical checkups and cancer screenings conducted at the Nagasaki Atomic Bomb Casualty Council Health Management Center. Details about the ABDI database were given previously.[17]

The LSS database was established in 1950, consisting of approximately 94,000 Hiroshima and Nagasaki atomic bomb survivors and 26,000 nonexposed city residents. Available data include information on exposure status, death and cancer diagnosis dates, and individual organ dose estimates computed by using the Dosimetry System 2002 (DS02).[18] The LSS database includes approximately 32,000 Nagasaki survivors. Details about the LSS database were given previously.[19]

Identification of MDS in Atomic Bomb Survivors

Of the 796 patients with MDS registered in the NPCR, 44 were excluded because of misdiagnosis and 147 were excluded because of residence outside the catchment area. The remaining 605 eligible patients with MDS were linked to the ADBI and LSS databases to identify atomic bomb survivors with MDS (ABDI-MDS and LSS-MDS, respectively). Follow-up for this study began in January 1985 when the FAB classification of MDS had been widely used in Japan. Figure 1 summarizes the patient selection process and provides information on the final cohorts used for analyses.

Statistical Analysis

We performed risk analyses only for those with known exposure distances or dose. Patients were limited to those with a definite or possible level of diagnostic certainty for MDS. Patients of therapy-related MDS (ICD-O-3 code 9987/3) or with an undetermined level of certainty were censored at the date of diagnosis. Follow-up began on January 1, 1985, and continued to the earliest of the date of the primary MDS diagnosis, death, or December 31, 2004. The

Table 1. Criteria for the Level of Diagnostic Certainty for MDS in Case Review

Level	Objective Evidence
Definite	Reaffirmation of dysmegakaryopoiesis and/or dysgranulopoiesis on the bone marrow aspirate smear.
	Bone marrow aspirate smear was not available, but there was a clear description of dysmegakaryopoiesis and/or dysgranulopoiesis on the medical record.
	Bone marrow aspirate smear was not available and there was no clear description of dysmegakaryopoiesis and/or dysgranulopoiesis, but there was a description of the presence of dysplasia in blood cells, myeloblast < 30%, and chromosome aberration on the medical record.
Possible	Morphologic evaluation was not available, but there was a clear clinical course from FAB-refractory anemia or refractory anemia with excess blasts to leukemia on the medical record.
Undetermined	Only the name of MDS was available on the medical record and the death certificate.

Abbreviations: MDS, myelodysplastic syndromes; FAB, French-American-British classification.

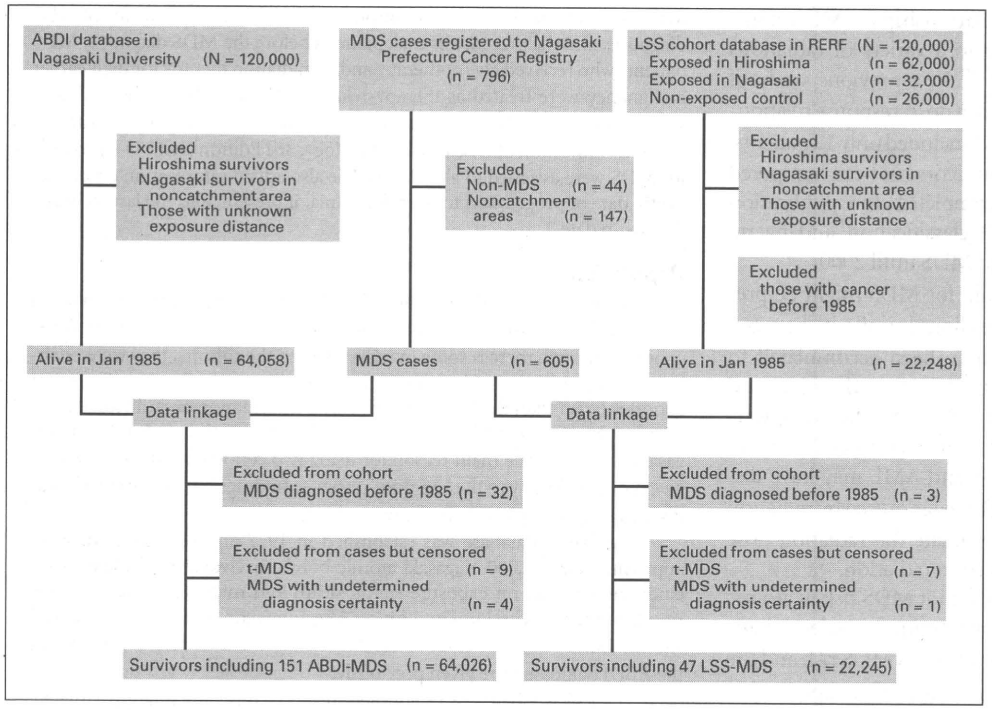

Fig 1. Study profile. ABDI, Atomic Bomb Disease Institute; MDS, myelodysplastic syndromes; LSS, Life Span Study; RERF, Radiation Effects Research Foundation; t-MDS, therapy-related MDS.

person-year calculations took into account date of migration in the ABDI data set, and a migration adjustment was made in the LSS data set. For the LSS data set, we also excluded those with cancer before 1985, and the follow-up was censored at the date of treatment with chemo- or radiotherapy for any cancer, if present, because all LSS cohort members are routinely linked to the NPCR. We treated patients with MDS either together, by FAB category, or by a dichotomized category of low-risk (RA and RARS) and high-risk (RAEB and RAEB-t).[20] We did not include CMML or "not otherwise specified" in the dichotomized category.

We used Cox regression models to estimate the effects of sex, age at exposure, exposure distance, and dose on MDS incidence rates. Relative risk (RR) estimates were computed by using SAS software (version 9.1; SAS Institute, Cary, NC). We used the asymptotic SEs as the basis for hypothesis tests and 95% CIs. Interactions between factors were also tested. We treated age at exposure as two (0 to19 and $\geq$ 20 years) or three groups (0 to 9, 10 to 19, and $\geq$ 20 years) or as continuous, as necessary, and exposure distance in km as three groups ($<$ 1.5, 1.5 to 2.99, and 3.0 to 10.0 km) or more detailed categories, and the weighted DS02 bone marrow dose in Gy as three groups ($<$ 0.005, 0.005 to 0.999, and $\geq$ 1 Gy) or as continuous. The cutoff values for exposure distance or dose were chosen on the basis of data from previous reports.[17,19,21] For categoric data, tests for independence or trend were carried out by using χ^2 or Fisher's exact tests, as appropriate. A two-tailed P value of $<$ 0.05 was judged significant.

We examined linear, linear-quadratic, and other dose-response functions for the LSS data adjusting for sex, age at exposure, and attained age or time since exposure, in a manner similar to earlier leukemia dose-response analyses,[6] and estimated the excess relative risk (ERR) per Gy by using weighted DS02 bone marrow dose. The basic ERR dose-response model can be written as BR $[1+ \alpha d]$, where BR is the baseline rate described as a parametric function of sex and attained age. We also examined ERR distance-response functions in the ABDI and the LSS cohorts with exposure distance treated as a continuous variable truncated at 3km (r[inf]3k) or with exposure distance categories of $<$ 1.25, 1.25 to1.49, 1.5 to1.74, 1.75 to1.99, 2.0 to 2.49, 2.5 to 2.99, and $\geq$ 3.0 km. The continuous exposure-distance model can be written as BR $[1 + \gamma \exp(-\beta r[\text{inf}]3k)]$ where the BRs are modeled as for the dose-response model, β is a distance-decay parameter, and γ is a scaling parameter. The distance-decay parameter value (x) is transformed to the percentage decrease in the ERR per km, which is calculated from the formula, $[1-\exp(-x)] \times 100\%$. ERR models were fit and likelihood-based P values and CIs were computed by using EPICURE software (Hirosoft International, Seattle, WA).[22]

RESULTS

The ABDI data set consisted of 64,026 Nagasaki atomic bomb survivors with information on exposure distance, including 151 ABDI patients with MDS who were diagnosed from 1985 to 2004. Of those, 147 (97%) were definite MDS patients and 4 (3%) were possible patients. The LSS data set consisted of 22,245 Nagasaki atomic bomb survivors for whom dose estimates were available. The 47 LSS patients with MDS included 45 (96%) definite and two (4%) possible patients. Table 2 presents the frequencies of FAB subtypes in both data sets. The distribution of subtypes in the ABDI and LSS cohorts did not differ (P = .54). The distribution characteristics, particularly the high frequency of RA relative to RARS and CMML, were typical for Japanese patients with MDS.[23] Cytogenetics data were available for 107 (71%) of 151 ABDI-MDS patients (Appendix Table A1, online only). The median age at exposure and the median age at diagnosis were 18.5 years (range, 0.3 to 43.4 years) and 71.0 years (range, 42.0 to 96.6 years) for ABDI-MDS, respectively, and 16.5 years (range, 2.5 to 48.8 years) and 72.4 years (range, 48.5 to 94.3 years) for LSS-MDS, respectively. The median time to development of MDS from 1985 was 12.0 years (range, 0.3 to 19.9 years) for ABDI-MDS and 14.5 years (range, 0.9 to 19.5 years) for LSS-MDS.

The total numbers of person-years in the ABDI and LSS cohorts were 947,215 and 270,619, respectively. The crude MDS incidence rates in the ABDI and LSS cohorts were 15.9 and 17.4 patients per 100,000 person-years, respectively. Table 3 summarizes the crude incidence rate and crude RR estimates by exposure status. MDS rates were higher for men than for women and increased with age at exposure. MDS rates also increased with decreasing distance from the hypocenter and with increasing estimated dose.

Table 2. Distribution of MDS by Exposure Distance or Dose in Two Cohorts of Atomic Bomb Survivors

Variable	Exposure Distance (km) for Nagasaki Atomic Bomb Disease Institute Cohort				DS02 Bone Marrow Weighted Dose (Gy) for Life Span Study-Nagasaki Cohort			
	< 1.5	1.5-2.99	≥ 3.0	Total	≥ 1	0.005-0.999	< 0.005	Total
Sex								
Male	1,693	6,485	16,092	24,270	273	2,665	5,904	8,842
Female	2,258	10,663	26,835	39,756	351	4,201	8,851	13,403
Total	3,951	17,148	42,927	64,026	624	6,866	14,755	22,245
MDS FAB subtypes								
RA	15	28	57	100	5	9	20	34
RARS	0	1	3	4	0	1	0	1
RAEB	7	8	14	29	2	3	2	7
RAEB-t	2	2	2	6	1	2	0	3
CMML	1	3	4	8	0	0	0	0
Unclassified	0	2	2	4	0	0	2	2
Total	25	44	82	151	8	15	24	47

Abbreviations: MDS, myelodysplastic syndromes; DS02, Dosimetry System 2002; FAB, French-American-British classification; RA, refractory anemia; RARS, RA with ringed sideroblasts; RAEB, RA with excess blasts; RABEB-t, RAEB in transformation; CMML, chronic myelomonocytic leukemia.

In Cox analyses for the ABDI cohort with adjustment for sex and age at exposure, the MDS incidence rate was significantly and inversely related to the exposure distance. The RR estimates for those exposed at < 1.5 and 1.5 to 2.99 km from the hypocenter were 2.8 (95% CI, 1.8 to 4.5; $P < .001$) and 1.3 (95% CI, 0.9 to 1.9; $P = .13$), respectively. Analyses of the LSS cohort also revealed that dose was a strong risk factor for MDS. Effects of exposure distance and dose on MDS were observed in both high-risk and low-risk MDS in both cohorts (Figs 2A and 2B). In a joint analysis of the dose and distance effects on MDS rates, there was a suggestion ($P = .08$) of larger radiation effects in high-risk MDS than in low-risk MDS. A significant linear dose association was observed in each risk group ($P < .001$). Effects of exposure distance and dose on MDS were also observed for those exposed before and after age 20 in both cohorts (Figs 2C and 2D). When we adjusted for attained age in 1985 in the ABDI cohort, age-specific MDS risks increased with increasing year of birth, with risks for those born after 1925 being about 1.75 (95% CI, 1.05 to 2.90) times the risks for those born in earlier years. The adjusted MDS risk using exposure dose in the LSS data showed similar results (RR, 1.71; 95% CI, 0.95 to 3.10). After allowing for birth cohort effects on the MDS risk, there was no evidence of a statistically significant interaction between distance or dose and age at exposure in either cohort (ABDI $P = .06$; LSS $P = .36$).

MDS rates decreased significantly with increasing distance for both cohorts ($P < .001$ for both). The fitted ERR curves were similar for the two cohorts. The decay parameters for ABDI and LSS cohorts were 1.2 per km (95% CI, 0.4 to 3.0) and 2.1 per km (95% CI, 0.6 to 4.6), respectively. In other words, the ERR is estimated to decrease by 70% per km (95% CI, 33% to 95%) in the ABDI and 88% per km (95% CI, 43% to 99%) in the LSS cohort. Figure 2E shows the fitted distance-response curves and point estimates of the distance category–specific ERRs with 95% CIs. There was a statistically significant ($P < .001$) linear dose-response for MDS in the LSS cohort with an ERR per Gy estimate of 4.3 (95% CI, 1.6 to 9.5; Fig 2F). A linear-quadratic model that fit the AML[6] did not improve the fit ($P = .46$).

DISCUSSION

To the best of our knowledge, this is the largest study to date evaluating the association between MDS risk and radiation exposure, and the first to provide quantitative estimates of the effect of radiation on MDS risk. We observed a significant ($P < .001$) linear relation between radiation dose and MDS risk among atomic bomb survivors with an ERR per Gy of 4.3. We also observed that the effect of radiation on MDS risk was greater in advanced subtypes of MDS and in those exposed at younger ages.

Our finding of a significant linear dose-response pattern for MDS is in contrast to the significant linear-quadratic dose-response pattern for AML.[6] The fact that the radiation-associated increases of MDS risk still exist 40 or more years after exposure is also in contrast to the risk of radiation-induced leukemia in which the largest dose-related increases were seen in the first 10 to 15 years after the bombings and then decreased slowly with time.[5,6] The linear dose-response pattern and the appearance with a long latency for MDS in atomic bomb survivors seems similar to those seen for radiation-associated solid cancers.[19]

Differences in the dose-response patterns for MDS and AML suggest that the nature of the radiation-induced genetic damages in hematopoietic stem cells may differ for the two diseases. Mutations in the *AML1/RUNX1* gene[24,25] may be one of the genetic damages associated with MDS that occurred in hematopoietic stem cells of atomic bomb survivors because of radiation exposure. Accumulating data on the different characteristics of the molecular and clinical spectrum, including chromosome aberrations between MDS and AML,[12,13,26-29] could shed some light on differences in the role of radiation exposure on these diseases.

Why is radiation-induced MDS seen in atomic bomb survivors more than 40 years after exposure? A primary reason for the long latency of MDS risk could be that atomic bomb survivors, even those exposed early in life, are reaching ages at which MDS rates are increased. In fact, in recent years, hematologists in Nagasaki City have identified an increasing number of MDS occurrences among atomic bomb survivors. Moreover, on the basis of the multistep pathogenesis